# THE DEVELOPMENT OF HYPOXIA ACTIVATED DNA REPAIR INHIBITORS

by

Kirstin Elizabeth Lindquist
BSc. Simon Fraser University, 2007

A THESIS SUBMITTED IN PARTIAL FULFILLMENT OF
THE REQUIREMENTS FOR THE DEGREE OF

MASTER OF SCIENCE

in

THE FACULTY OF GRADUATE STUDIES
(Pathology and Laboratory Medicine)

THE UNIVERSITY OF BRITISH COLUMBIA
(Vancouver)

November 2009

# Abstract

The human body's vast network of blood vessels provides oxygen and nutrients throughout the body, however hypoxic cells (cells with lower than normal physiological oxygen levels) are found in human tumours. Hypoxic cells are resistant to ionizing radiation and therefore are an impediment to the effectiveness of radiotherapy. Ionizing radiation kills cells by causing DNA damage; the principal lethal lesion formed is the DNA double strand break (DSB).

This work concerns the development of a hypoxia activated DNA repair inhibitor prodrug. The specific target of the prodrug is a critical DSB repair enzyme of the non-homologous end joining pathway (NHEJ), called DNA dependent protein kinase (DNA-PK). This work concerns the development of pharmaceutical screening tools for agents that act as radiosensitizers of oxic and hypoxic cells. These tools were then used to demonstrate that DNA-PK deficiency can sensitize hypoxic mammalian cells to the effects of ionizing radiation, and that 2-nitroimidazole derivatives of the DNA-PK inhibitor IC86621 cell-based screening results from hypoxia activated DNA repair inhibitors that display hypoxia selective radiosensitization of CB.17 murine embryonic fibroblast and HeLa human cervical carcinoma cells.

# Table of contents

# List of tables

# List of figures

# Acknowledgements

Foremost I would like to acknowledge my supervisor throughout this project, Dr. Andrew Minchinton, whose innovation, mentorship, and encouragement made this work possible.

I would like to thank Dr. Alastair Kyle whose brilliance in the laboratory and contribution to this work is difficult to overstate. Dr. Kyle's dedication to his work, creativity, skilfulness and willingness to help others constantly inspire me.

A special thanks to Dr. Robyn Seipp who carried out the flow cytometry experiments and was a joy to work with on this project.

Also a thank-you to my former and present lab mates Dr. Lynsey Huxham and Jennifer Baker. Lynsey who mentored me patiently when I was a young naïve co-op student and Jenn who has been an understanding friend and lab mate over the years.

Lastly I would like to thank the many co-op students whose hard work contributed to the work presented in this thesis, particularly Misa Noda and Jordan Cran.

## Dedication

This work is dedicated to *my parents* *Gordon and Elizabeth Lindquist* for their **unwavering commitment** and support of my education AND to *my best friend and partner* *Scott Yuzwa*, whose **laughter, love & encouragement** made this work possible on even the **darkest rainiest** Vancouver days.

# Glossary

| | |
|---|---|
| γH2AX | Variant of histone H2A phosphorylated at serine residue 139. |
| λ | Light wavelength |
| μM | Micromolar |
| ARCON | Accelerated radiotherapy, carbogen and nicotinamide |
| ATM | Ataxia telangiectasia mutated |
| ATR | Ataxia telangiectasia and Rad3 related |
| DNA | Deoxyribonucleic acid |
| dsDNA | Double stranded deoxyribonucleic acid |
| DNA-PK | Deoxyribonucleic acid dependent protein kinase |
| DNA-PKcs | Deoxyribonucleic acid dependent protein kinase catalytic subunit |
| D-PBS | Dulbecco's modified phosphate buffered saline |
| DSB | DNA double strand break |
| ECL | Enhanced chemiluminescence |
| Gy | Gray: one gray is the absorption of one joule of energy, in the form of ionizing radiation, by one kilogram of matter. |
| h | hours |
| H2A.X | The X variant of histone H2A |
| HIF1-α | Hypoxia inducible factor 1 alpha |
| HRP | Horseradish peroxidase |
| HRR | Homologous recombination repair |

| | |
|---|---|
| IC50 | Half maximal inhibitory concentration: The concentration of a substance necessary to inhibit enzymatic activity by 50% |
| IR | Ionizing radiation |
| kDa | Kilodaltons |
| min | Minutes |
| mM | Millimolar |
| mm | Millimeter |
| mTOR | Mammalian target of rapamycin |
| NADPH | Nicotinamide adenine dinucleotide phosphate |
| NHEJ | Non-homologous end joining |
| OER | Oxygen enhancement ratio |
| p110$\alpha$ | Phosphotidylinositol-3-Kinase p110 alpha |
| p110$\beta$ | Phosphotidylinositol-3-Kinase p110 beta |
| p110$\gamma$ | Phosphotidylinositol-3-Kinase p110 gamma |
| p110$\delta$ | Phosphotidylinositol-3-Kinase p110 delta |
| PBST | Dulbecco's modified phosphate buffered saline containing 0.01% polysorbate 20 (commercially known as Tween-20) |
| $pCO_2$ | Partial pressure of carbon dioxide |
| PHD | Prolyl hydroxylase |
| PIKK | Phosphotidylinositol-3-kinase like kinase |
| PI3-K | Phosphotidylinositol-3-kinase |
| $pO_2$ | Partial pressure of oxygen |
| *prkdc* | Protein kinase, DNA-activated, catalytic polypeptide. This gene encodes the DNA-PKcs transcript. |
| s | Seconds |

| | |
|---|---|
| SCID | Severe combined immunodeficiency |
| SDS-PAGE | Sodium dodecyl sulfate polyacrylamide gel electrophoresis |
| TLD | Thermoluminescent dosimetry |
| XLF | XRCC4-like factor |
| XRCC4 | X-ray repair cross complementing protein 4 |

# Chapter 1: Introduction

## 1.1 Hypoxia and radiation therapy

Radiotherapy is a mainstay in the treatment of many types of cancer, however the efficacy of radiotherapy is limited by the damage caused to normal tissues surrounding the tumour volume. At doses given clinically, radiation resistant populations of hypoxic cells that exist within the tumour microenvironment reduce the ability of radiotherapy to cause the formation of highly reactive radical species within cells. These radical species result in multiple forms of cellular damage including protein-protein and protein-DNA cross-links, as well as various forms of DNA damage (1). The most lethal lesions caused by radiotherapy are DNA double strand breaks (DSB), in which both strands of a DNA double helix are severed within 15-20 base pairs (2). The importance of DSB is evident in the close correlation between the number of DSB generated by ionizing radiation and the resulting cell death, and additionally by the severe radiosensitivity resulting from loss-of-function mutations in genes which code for proteins involved in DSB repair pathways (3, 4).

### The oxygen effect

The presence of molecular oxygen is thought to potentiate the effect of ionizing radiation by a mechanism described in the oxygen fixation hypothesis (5). The oxygen fixation hypothesis maintains that the critical product of radiation, DNA radicals, can be oxidized by cellular molecular oxygen to form enzymatically irreparable peroxyl-DNA adducts (5). According to this hypothesis, hypoxia renders cells resistant to the effects of ionizing radiation owing to the low concentration of molecular oxygen available to oxidize

the DNA radicals and the presence of a cellular environment that is more conducive to the reduction of DNA radicals by thiol containing compounds, such as glutathione. When molecular oxygen is scarce, thiol containing compounds are thought to effectively compete for reduction, rather than oxidation of the DNA radicals, resulting either directly in restitution of the DNA structure or in a form of damage amenable to repair cellular DNA repair enzymes (2). The cell survival difference observed between cells irradiated under well-oxygenated and hypoxic conditions is commonly quantified by a term called the oxygen enhancement ratio (OER). OER is defined as the ratio of the hypoxic and oxic doses of radiation required to produce a given surviving fraction of cells. The OER varies modestly between cell lines and reaches a maximum value close to 3.0 (6).

## 1.2 DNA double strand break repair

**Homologous recombination repair**

The mammalian cell has two primary pathways used to repair DNA double strand breaks: homologous recombination repair (HRR) and non-homologous end joining (NHEJ). HRR is a high fidelity, potentially error-free repair pathway that uses a DNA strand with long regions of homology to the damaged region, normally a sister chromatid, as a template for repair. This involves recognition of the DNA damage by sensor proteins, followed by endo/exonuclease processing of the damaged strands which allows for invasion of the damaged strand into the template strand and subsequent replication of the damaged strand using the intact template (7). Although HRR can be a high fidelity DSB repair pathway, the requirement for a homologous strand to be in close proximity to the DSB restricts its activity to the S and $G_2$ phases of the cell cycle (8). It can be argued that since HRR is limited to cells within S and $G_2$ phase, targeting HRR could provide a therapeutic index by damaging the actively proliferating cancer cells while having less effect on most normal quiescent tissue.

Problems could arise however when targeting HRR in chronically hypoxic cells because a key protein of the HRR pathway, Rad51, has been found to be down regulated in chronically hypoxic cells and this deficiency in Rad51 has been found to limit the use of the HRR pathway in hypoxic cells (9-11). Additionally, loss-of-function mutations in proteins involved in HRR increase sensitivity to X-rays, but more severe radiosensitivity occurs in response to X-rays when components of the NHEJ pathway are deficient, implicating NHEJ as the predominant pathway involved in repair of ionizing radiation induced damage (12).

**Non-homologous end joining**

NHEJ is a low fidelity DSB repair pathway in which the ends of a DSB are detected by DNA damage sensor proteins in a similar manner to HRR, however in NHEJ the DNA ends are processed by endo/exonucleases and DNA polymerases into a suitable substrate for ligation. In contrast to HRR, this process occurs without the use of a homologous DNA template strand and inevitably leaves insertion and/or deletion mutations flanking the repaired region. In NHEJ the sensor proteins are two units of a ring-shaped heterodimeric protein complex called Ku70 and Ku80. The Ku proteins bind with high affinity to the ends of dsDNA, with very minimal to no selectivity for DNA sequence or structure (13). The large 470kDa catalytic subunit of the DNA dependent protein kinase (DNA-PKcs) is then recruited to each of the Ku 70/80-DNA complexes (7). The entire holoenzyme complex of DNA, Ku 70/80, and DNA-PKcs is referred to as DNA-PK. Once formed, DNA-PK becomes activated by multiple autophosphorylation events, the specific details of which are yet to be well characterized. It is clear that this activation initiates movement of the DNA-PK complex away from the broken ends, allowing for recruitment of processing enzymes, such as the endonuclease artemis, and a ligation complex composed of XLF, XRCC4, and ligase IV (12). Mutagenesis of DNA-

PKcs at amino acid residues that are known to be autophosphorylated diminishes NHEJ activity and can either inhibit or enhance the HRR pathway depending on the region mutated, demonstrating the crucial role of DNA-PK activation in DBS repair (14).

DNA-PKcs is a member of the PI3-Kinase-like Kinase (PIKK) family of proteins, which also includes other DNA damage responsive proteins, ATM, ATR, and mTOR (15). Members of the PIKK family have a characteristic catalytic domain bearing sequence homology to that of the lipid phosphotidylinositol 3-kinases (15). Structural information is limited for DNA-PKcs due to the lack of a high-resolution X-ray crystal structure or solution NMR structure. Difficulty obtaining such structures is likely because of the proteins large 470 kDa size. Despite this lack of structural information, selective inhibitors of DNA-PKcs have been developed based on homology modelling with the crystal structure of PI3-K and pharmacophore mapping of the non-selective inhibitor LY294002 (16, 17).

## 1.3 Hypoxic cell radiation sensitizers and hypoxia activated prodrugs

A number of treatment approaches and anti-cancer agents have and continue to be designed to target hypoxic cells in solid cancers, including many trials of hyperbaric oxygen, hypoxic cell radiosensitizers, bioreductive hypoxic cytotoxins, carbogen, and accelerated radiotherapy with carbogen and nicotinamide (ARCON) (18). Aside from select hypoxic cytotoxins currently undergoing clinical evaluations, most of these agents or modalities have had disappointing results due to high toxicity profiles or impracticality, and have been stymied by an inability to select appropriate patient populations that would most benefit from treatment. Despite the disappointing results of individual trials, meta-analysis of multiple clinical trials of nitroimidazole based agents and the hyperbaric oxygen trials suggests that targeting the hypoxic cell population is a valid strategy and

can enhance both local tumour control and patient survival, particularly in patients with head and neck, bladder, and uterine cervix cancers (19-22).

The nitroimidazole based hypoxic cell radiosensitizers are sometimes referred to as oxygen mimetic radiosensitizers because there are some parallels with oxygen in their reactivity towards DNA base radicals (23). The exact mechanism of action of these agents is somewhat unclear due to the short half-life of reactive intermediates, but it is thought to involve the generation of DNA strand breaks through a fixation of DNA damage, as well as reaction with protein thiols and DNA bases to form detrimental macromolecule-drug adducts (23-25). As radiosensitizers, nitroimidazole drugs require very high peak serum concentrations in order to be effective. For example, in humans a 0.5-4 g dose of misonidazole (Ro 07-0582) is required such that peak plasma concentrations reach to the order of 0.1-1 mM (26). Similarly, in order to sensitize hypoxic cells in culture such that they become similar in radiosensitivity to oxygenated cells, >15 mM misonidazole in cell culture media is required (27). In this work, some of the prodrugs utilize a nitroimidazole as the basis for a hypoxia activated trigger, however the concentration of prodrugs administered is up to 150x lower than that of misonidazole in culture because the radiosensitizing activity of these prodrugs is derived from a more potent and molecularly targeted DNA-PK inhibitor.

The components of a prototype prodrug and mechanism of prodrug activation are displayed in figure 1.1. We have taken a modular approach to the design of hypoxia activated DNA repair inhibitors (HADRI) prodrugs, as first described by Denny et al. (28). In this approach, prodrug design is considered with regard to three modules, those being 1) a trigger, which is required to undergo selective activation in tumour cells, 2) a linker, which is required to deactivate the effector and transmit the trigger activation signal, 3) an effector component, which exerts a potent cytotoxic effect. With this design, the

nitroimidazole acts as a means for hypoxia selective bioreduction, defining it as the trigger component of the prodrug. The prodrugs developed herein are designed to undergo intramolecular through-bond fragmentation upon bioreduction in hypoxic tissue. This mechanism has been previously described for prodrugs containing nitroaromatic triggers, and involves a four electron reduction of the nitroaromatic into a hydroxylamine (29). For the prodrugs described herein, this reduction is designed to result in fragmentation of a strategically placed ether linker, releasing the effector, a potent DNA-PK inhibitor. By including a DNA-PK inhibitor as the effector module of these prodrugs, we hope to prevent DNA repair in the hypoxic regions of tumours following radiotherapy. It is hoped that this design will dramatically increase the potency of these prodrugs over that of previous hypoxic cell radiosensitizers, thereby requiring lower doses for effective treatment and lessening the systemic toxicity.

## 1.4 Current status of DNA-PK inhibitors for use in cancer treatment

In contrast to nitroimidazole based hypoxic cell radiosensitizers, which have undergone many clinical trials, DNA repair inhibitors have been developed more recently and entered clinical trials in 2005 with inhibitors of a DNA single strand break repair protein called poly (ADP-ribose) polymerase or PARP. PARP inhibitors are showing early success, particularly in treating patients with hereditary breast ovarian cancer syndrome where tumours carry mutations in both copies of the DNA repair associated BRCA1 and BRCA2 genes (30). Inhibitors of the DSB repair proteins ATM, a critical protein in the HRR pathway, and DNA-PK are also being developed for therapeutic use in cancer and are currently in various stages of pre-clinical development (7, 31-36).

We have chosen a DNA-PK inhibitor called IC86621 as the focus of our initial proof of principle and drug development studies; see Appendix C for chemical structure.

Although IC86621 is designed to target NHEJ through the inhibition of DNA-PK, it has been shown that treatment with IC86621 also decreases the amount of HRR repair (37, 38). It is suspected that inhibition of DNA-PK using the ATP competitive inhibitor IC86621 or the non-competitive inhibitor wortmannin stalls the DNA-PK complex at the site of a DSB by disallowing DNA-PK autophosphorylation (37). With DNA-PK stalled at the broken DNA ends, the access of other repair proteins to the site of the break is restricted.

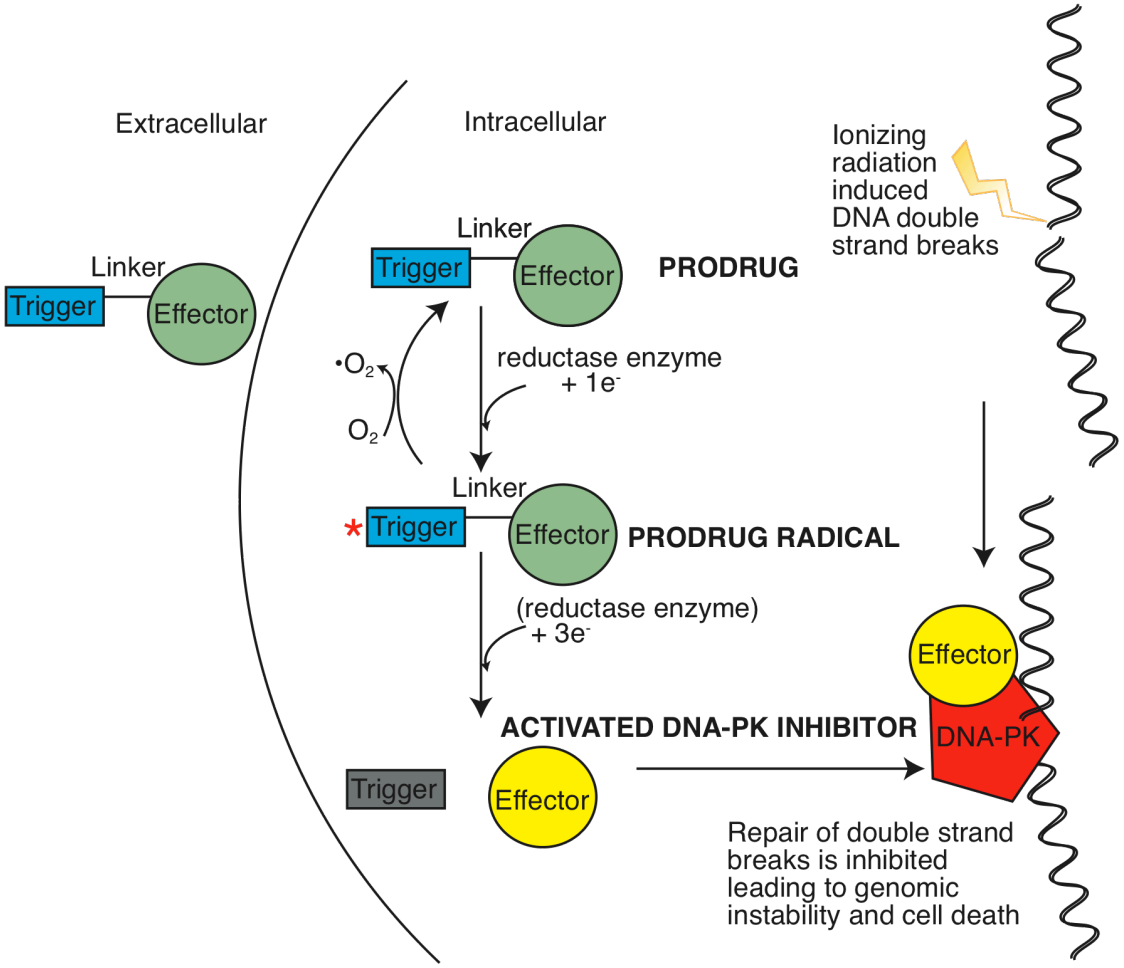


**Figure 1.1 Mechanism and components of hypoxia activated DNA repair inhibitor prodrugs**
The modular components of hypoxia activated DNA repair inhibitor prodrugs include a nitroaromatic trigger, an ether linker, and a DNA-PK inhibitor effector. The compound is inactive in its prodrug form, however upon entering cells it is bioreductively activated in the absence of molecular oxygen. This bioreductive activation occurs by the nitroaromatic trigger acting as a substrate for a one electron reduction by a nitroreductase enzyme, such as P450 reductase, which produces a prodrug radical. This prodrug radical can then be quickly back oxidized by molecular oxygen to reproduce the original prodrug leaving behind a superoxide radical. In hypoxic conditions where molecular oxygen is not abundant to back oxidize the prodrug radical, the compound will be further reduced. Once a four electron reduction of the original compound has occurred, the covalent bond between the ether linker and the effector will break, releasing the activated DNA-PK inhibitor. In hypoxic tumour cells that have sustained DNA damage from the administration of radiation therapy, the DNA-PK inhibitor will disallow repair of DNA double strand breaks, resulting in cell cycle arrest and cell death.

# Chapter 2: Materials and methods

## 2.1 Hypoxia and radiation treatments

For hypoxia treatments, cells plated on glass were placed into a custom-built aluminium chamber, described in detail in chapter 3, which was then sealed and equilibrated to the desired gas mixture through cyclic evacuation and pressurization of the chamber with constant bilateral agitation of the culture media. This protocol is similar to that described previously (39). Briefly, the process consisted of eight 1 min cycles of 1) evacuation to 46.5 centimetres of mercury (cm Hg) vacuum over 5 s, 2) holding this vacuum for 20 s, 3) release of the vacuum over 5 s, 4) pressurization to 25.8 cm Hg over 5 s, 5) holding the pressure for 20 s, 6) release of the pressure over 5 s, which completes one cycle. Pressure is described in reference to standard atmospheric pressure being zero (gauge pressure). After eight cycles, a final cycle with the same evacuation procedure followed by pressurization to 5.2 cm Hg was completed and the chamber was left to agitate for 1 min. The total time used to reach radiobiological hypoxia was 10.3 min. This procedure was shown to be non-toxic to cells, however for experimental control, all cells in both oxygenated and hypoxic conditions were treated with this gassing procedure, using mixtures of 0-20% $O_2$, 5% $CO_2$, 95-75% $N_2$ (Praxair). X-ray irradiation was delivered to the aluminium chambers with a 300 keV Pantak Siefert XRAD320 irradiation system at 3.3 Gy/min with no filtration other than that produced by the chamber (5 mm aluminium).

## 2.2 Inhibitors, drugs and prodrugs

1-(2-Hydroxy-4-morpholin-4-yl-phenyl)ethanone (IC86621) was synthesised in the laboratory of Dr. Gregory Dake, University of British Columbia Department of Chemistry according to previously published methods (40). A stock solution of 15 mg/mL IC86621 in DMSO was prepared and small volume aliquots were prepared to avoid freeze thaw cycles. Aliquots were stored in the dark at -20 °C. The laboratory of Dr. Gregory Dake at the University of British Columbia Department of Chemistry synthesized HADRI1, HADRI2, HAPI2, and IC86621, the structures and IUPAC names for which are listed in appendix C. HAPI3 was synthesized by Geoff Winters at the Centre for Drug Research and Development (Vancouver, BC). 2-(Morpholin-4-yl)-benzo[h]chomen-4-one (NU7026) was purchased from Sigma-Aldrich Canada Ltd(catalogue no. N1537) A stock solution of 3 mM NU7026 in DMSO was prepared and similarly stored in small aliquots away from light at -20 °C. Hydroxy-3H-phenoxazin-3-one-10-oxide sodium salt (Resazurin, Sigma-Aldrich Canada Ltd, R7017) was prepared as a 2.2 mM stock solution in 0.9% NaCl. Resazurin was prepared in a biosafety cabinet and sterile filtered through a sterile 0.2 μM filter (Sarstedt Inc, 83.1826.001). The sterile resazurin stock solution was stored away from light at 4 °C.

## 2.3 Cell culture

CB.17 and SCID/st mouse embryonic fibroblast cell lines, M059K and M059J human glioma cells, and HeLa human cervical carcinoma cells were a gift from Dr. Peggy Olive. All cells were maintained in vented cap cell culture flasks (Sarstedt Inc, 83.1810.002, 83.1812.002, 83.1813.002) with Minimum Essential Medium with Earle's buffered salt solution (MEM/EBSS, Hyclone, Thermo Scientific, SH30013.03) supplemented with 10% fetal bovine serum (FBS, Hyclone, Thermo Scientific or Gibco,

Invitrogen). In some experiments antibiotics were included in the media, 50 mg/mL penicillin and 50 U/mL streptomycin (Gibco, Invitrogen). For the purpose of this thesis, standard incubation conditions include a humidified incubator at 37 °C in a 5% $CO_2$/ 5% $O_2$/ 90% $N_2$ atmosphere and any referral to cell culture media or medium, unless otherwise stated, refers to MEM/EBSS containing 10% FBS.

## 2.4 Resazurin reduction assay

This assay has been previously described for use in assessing cell viability following exposure to ionizing radiation(41). Exponentially growing cells were harvested using trypsin (Sigma-Aldrich Canada Ltd, T4049) and counted by haemocytometer. Cells were then seeded into 1.5 cm diameter custom made glass tissue culture inserts fitted for standard non-treated 24 well plates (BD Biosciences, 351147) at a density of 5 x $10^3$ cells/well (CB.17) or 7.5 x $10^3$ cells/well (HeLa). After seeding, cells were incubated in standard conditions for 18-24 h with 500 μL of medium/well. After 18 h the medium was removed and replaced 1 h pre-irradiation, by 200 μL of medium containing DMSO, DNA-PK, or prodrugs as specified. 24 well plates were placed into aluminium chambers and gassed and irradiated as described in section 2.1. As specified, between 0-6 h following irradiation plates were removed from the chambers and placed back under standard incubation conditions. Drug treatments remained on the cells for 4-24 h following irradiation as specified, at which point the medium was replaced with 500 μL of fresh medium. In all experiments, 72 h following irradiation a stock solution of 2.2 mM resazurin was added to the cell culture medium to a final concentration of 220 μM. Approximately 4-8 h following the addition of resazurin, when the medium within the untreated control wells turned a dark pink colour, the amount of reduced resazurin (resorufin) was assayed by fluorescence using a TECAN GENios plate reader, excitation

λ535 nm, emission λ590 nm. Percent viability was determined by normalizing fluorescent values such that the mean resorufin fluorescence of non-irradiated controls represents 100% viability and the background fluorescence from 220 μM resazurin in cell culture medium without cells represents 0% viability. Graphs were generated with Prism 4.0 (GraphPad Software Inc.).

## 2.5 Clonogenic survival assay

For clonogenic survival assays 1 x $10^5$ HeLa cells were plated into 1.5 cm diameter custom glass inserts in non-treated 24 well plates (BD Biosciences, 351147), or 2 x $10^6$ CB.17 or SCID/st cells were seeded in sterilized 60 mm diameter glass petri dishes (VWR International, 89000-300). Cells were incubated under standard incubation conditions for 18-24 h before use in experiments. For drug treatments in section 4.4, HeLa cells were pre-incubated for 1 h before irradiation with 100 μM IC86621, 100 μM HADRI1, or 0.1% DMSO as a vehicle control. Drug treatments remained on the cells for 4 h following irradiation, making for a 5 h total drug exposure time. Immediately following irradiation (CB.17 and SCID/st cells) or drug removal (HeLa cells), cells were harvested by trypsinization and kept on ice before being counted with a Z1 Coulter particle counter (Beckman Coulter). Dilutions were made in media such that approximately 100 surviving colonies would result, and cells were plated on standard 60 mm and 100 mm diameter tissue culture dishes (BD Falcon) with 10 mL media. Cells were incubated in standard conditions for 10-14 days before the media was removed and surviving colonies were stained with 1% crystal violet / 30% ethanol solution. Colonies of >50 cells were counted and the surviving fraction was determined by the following formula:

$$\text{Surviving fraction} = \frac{\text{number of cells plated x plating efficiency}}{\text{number of colonies}}$$

## 2.6 Flow cytometry of γH2AX and cell cycle analysis

1.5-2 x $10^6$ HeLa cells were plated in 60 mm glass dishes and incubated overnight in a 5% $O_2$/ 5% $CO_2$ incubator. The following day plates were pre-treated for one hour with 100 μM IC86621 or 0.1% DMSO in media. Cells were then gassed and irradiated as described in section 2.1. Following irradiation cells remained in the chambers at a given oxygen tension at 37 $^oC$ for one hour and were then removed to normal incubation in a 5% $O_2$/ 5% $CO_2$ incubator for a further 23 h. Cells were harvested 24 h following irradiation, fixed in methanol and stained for flow cytometry with a monoclonal antibody to γH2AX (Upstate mouse mAb anti-phospho H2AX Ser 139 clone JBW301), either directly conjugated to fluorescein isothiocyanate (FITC) or by using an AlexaFluor 488 anti-mouse secondary antibody (Invitrogen). The same cells were also treated with 5 mg/mL RNase A and stained with 50 mg/mL propidium iodide (Sigma, P4170) for cell cycle analysis. Results were analyzed with FlowJo software (Tree Star Inc.) using the Dean/Jett/Fox cell cycle algorithm.

## 2.7 Mouse liver microsome preparation

This protocol is a modified version of that described by Wu and McKown (42). Mouse liver mircosomes were prepared using livers from 10 week old male C57/Bl6 mice. Following euthanasia by $CO_2$ asphyxiation, livers were excised and rinsed briefly in sterile 0.9% NaCl. Tissue was minced with a scalpel and homogenized in a dounce homogenizer with the addition of 2-4 mL/liver ice cold Tris-HCl buffer (1.15% KCl, 0.05 M Tris-HCl pH 7.4). The liver homogenate was divided into equal volumes in ultracentrifuge tubes (Ultra-clear open top, Beckman Coulter) and the volume of liquid within the tubes was brought to 38 mL with Tris-HCl buffer. The liver homogenate was then centrifuged at 9,000 xg in an SW28 rotor (Beckman Coulter) for 30 min at 4 °C. The

resulting supernatant (S9) was then transferred to fresh ultracentrifuge tubes and brought to 38 mL volume with Tris-HCl buffer. The S9 was then centrifuged for 1 h at 100,000 xg at 4 °C. The supernatant was then discarded and the resulting microsomal pellet was re-suspended in 1 mL per liver cold 0.1 M HEPES/ 1.15% KCl buffer. Aliquots of microsomes were stored at -80 °C until use. Protein concentration of the microsome solutions was determined to be 20 mg/mL by the Biorad DC Assay.

## 2.8 Microsomal stability assays

This protocol is modified from that of Lan et al. (43) Microsomal incubations occurred in a total volume of 0.5 mL containing 5 μL of 0.5 M MgCl (5 mM MgCl final), 50 μL of 20 mM nicotinamide adenine dinucleotide phosphate (NADPH, Sigma, N6505) (2 mM NADPH final), 10 μL of microsomes (200 μg protein), and either 420 μL of 178 μM HAPI3 (150 μM HAPI3 final) or 1.19% DMSO (1% DMSO final) in Dulbecco's phosphate-buffered saline (D-PBS, Hyclone). Microsomes were added last to start the reaction and experimental controls in which NADPH and/or microsomes were replaced with distilled $H_2O$ were performed in parallel. Reactions were incubated at 37 °C in either room air or in a hypoxic glove box at 0.2 ± 0.2% $O_2$ for 2 h. 50 μL samples were removed from reactions every 20 min. Reactions were stopped by the addition of 200 μL ice cold methanol. Samples were stored at -20 °C for 1-2 days before HPLC analysis was performed.

## 2.9 High pressure liquid chromatography (HPLC)

Chromatographic analysis was performed on Waters HPLC equipment (Waters Limited, Mississauga, ON, CA), including a model 510 pump, model 712 WISP injector, and model 996 photodiode array detector. A Symmetry C18 column (3.9 x 150 mm) was

used for sample separation with a mobile phase consisting of a mixture of 36% acetonitrile flowing at 1.5 ml/min where by HAPI3 eluted after 3.6 min and IC86621 after 4.6 min. Samples of 30 μL were injected and detection was carried out at λ320 nm for HAPI3 and λ340 nm for IC86621. Concentrations were determined from absorbance values using standard curves of external standards.

## 2.10 Cell lysis and western blotting

1-5 x $10^6$ HeLa cells were plated in 10cm diameter standard tissue culture dishes (Sarstedt) and were incubated in standard conditions for 24-72 h before being placed in a humidified 37 °C incubator within a glove box containing 1% $O_2$/ 5% $CO_2$/ balance $N_2$ for 4-72 h. Cell lysis occurred within the glove box by removing the culture media, rinsing the plates once with D-PBS, and adding 1.5 mL of Mammalian Protein Extraction Reagent (M-PER, Pierce, Thermo Fisher Scientific) containing 1 mM Sodium Fluoride, 1 mM Sodium Orthovanadate, 2 mM phenylmethanesulphonylfluoride (PMSF) and 10 μL/mL Protease Inhibitor Cocktail (BioShop Canada Inc, SFL001, SOV664, PMS123, PIC004). Cells were scraped into the 1.5 mL of lysis buffer and the volume from each plate was collected into a 1.5 mL tube (Sarstedt). Cell solutions were shaken in the hypoxic glove box following and protein concentration was determined using the Biorad DC Assay (BioRad Laboratories Canada Ltd.). For western blots, 100 μg lysate samples in Laemmelli buffer were separated by discontinuous sodium dodecyl sulfate polyacrylamide gel electrophoresis (SDS-PAGE) and electroblot transferred to 0.45 mM nitrocellulose membrane using the mini-PROTEAN 3 system (Bio-Rad Laboratories Canada Ltd). Membranes were blocked for 1 h with 2% bovine serum albumin (BSA) in PBST buffer (D-PBS containing 0.01% Tween-20) before being incubated with primary antibodies against Ku70 (mouse anti-Ku70, Santa Cruz Biotechnology, Ab-9), Ku80 (mouse anti-Ku80, Neomarkers Thermo Scientific, Ab-2), DNA-PKcs (rabbit anti-DNA-

PKcs, Calbiochem, Ab-1), and β-tubulin (mouse anti-β-tubulin, Invitrogen). Following washing 5x in PBST over 1h, secondary antibodies solutions of horseradish peroxidase (HRP) conjugated goat anti-mouse (Invitrogen, 65-6420) or goat anti-rabbit (AbCam, ab6721-1) were applied to the membranes. Membranes were again washed 5x in PBST over 0.5 h before the addition of enhanced chemiluminescence (ECL) detection reagents (Thermo Scientific).

# Chapter 3: Development of prodrug screening assays

Preliminary drug discovery screening assays can be broadly broken down in to two categories, cell-based screening assays that measure the activity of test compounds on cell cultures, and cell-free *in vitro* assays that measure the ability of test compound to directly affect the pathway or protein target of interest in a biochemical assay. The benefits of these assays are complementary and when both are used, they allow for assessment of drug activity and cellular toxicity in the complex milieu of the cell and a more mechanistic understanding of effects on the specific protein target. This chapter describes the development of both cell based and cell-free assays that have been designed to screen candidate hypoxia activated DNA repair inhibitor prodrugs. A focus has been deliberately placed on the cell-based assays, as these have had to be developed in house to be used as the primary screening tool, while commercial assays are readily available for *in vitro* assessment of DNA-PK kinase activity.

## 3.1 Hypoxia chamber development: the effect of cyclic evacuation and pressurization on cell viability

### Introduction

In order to develop hypoxia activated radiosensitizing agents in an efficient and economical manner, it was necessary to develop a series of screening assays that employ systems for rendering cells hypoxic whilst allowing them to be irradiated. Many groups studying hypoxia perform cell culture based experiments within sealed plexi-glass glove boxes, wherein cells can be manipulated within the glove box, but cannot be easily transported out of the glove box while remaining hypoxic. Furthermore, performing

experiments in which multiple oxygen tensions are tested can take many days in a glove box due to the lengthy time required for gases to exchange throughout the large volume of the box. To circumvent these problems, custom hypoxia chambers were designed and constructed by Dr. Andrew Minchinton and Dr. Alastair Kyle, in which cells can be rapidly rendered hypoxic due to the small volume of the chamber. This smaller chamber is also easily transportable, making possible transfer to an X-ray machine for irradiation. A diagram and photograph of the chamber can be seen in figure 3.1. The design of this chamber is based upon that of a similar aluminium hypoxia chamber previously described by Dr. Cameron Koch (39, 44).

Earlier efforts using aluminium hypoxia chambers involved a relatively slow gas exchange process in which the gaseous contents of the chamber were exchanged between 5-8 times over the course of 1-48 h (44-46). In aluminium hypoxia chambers, evacuation at reduced pressure causes rapid out-gassing of residual cellular oxygen, while using a thin medium layer allows rapid equilibration with the replacement gas mixture. Seeing as mild positive and negative pressure cycles had no effect on cell viability in these systems, we used a wider range of gauge pressure within the gas exchange cycles, including pressurization to 25.8 cm Hg and vacuum to 46.5 cm Hg. This gas exchange protocol was tested by examining cell viability 72 h following a 10.3 min gas exchange procedure with 21% $O_2$/ 5% $CO_2$ / balance $N_2$ gas.

**Approach**

HeLa human cervical carcinoma cells were plated on glass inserts within 24 well plates as per section 2.4. In this experiment control cells were not treated to the gas exchange procedure, but were left in laboratory atmosphere conditions for 10 min. The viability of control cells was compared to cells that had been gassed using our standard gassing protocol of eight 30 s evacuation/ 30 s pressurization gas exchange cycles in

the aluminium chamber with 21% $O_2$/ 5% $CO_2$/ balance $N_2$. Non-irradiated cells were placed immediately back in to standard incubation conditions following the 10 min wait or the 10 min gas exchange procedure, while irradiated cells were placed back in standard incubation conditions immediately following irradiation. Irradiated cells received a dose of 5 Gy immediately following either the 10 min wait period in air or following the 10 min gassing protocol. A minimum of n = 24 wells for each treatment group and an unpaired two-tailed t-test analysis was performed on the groups using Prism GraphPad V5.0b for Macintosh software. A P-value <0.01 was considered to be significant. Cell viability was assayed with the resazurin reduction assay 72 h following treatment as per section 2.4.

**Results**

Figure 3.2 displays the results of a cell viability assessment following the gas exchange procedure. Contrary to our expectation of some toxicity imposed by the gassing, the gas exchange protocol confers a slight but significant increase in viability over cells left outside of the incubator in normal air for 10 min ($P<0.05$, two tailed unpaired t-test). Although the cause of this increase was not further investigated, it may be due to appropriate buffering of the media with 5% $CO_2$ during the gassing protocol, while the cells left in atmospheric air may become somewhat alkaline due to the low $pCO_2$ in atmospheric air. This effect on cell viability becomes indiscernible in cells treated with 5 Gy IR, as there is no significant difference found in viability between cells that were irradiated following gas exchange or following 10 min in laboratory air. Despite only minor effects of cell viability, in attempt to rule out any effects on survival caused by the gassing protocol, all cells were treated with the gas exchange protocol in both control and treatment groups for all of the experiments in this work unless otherwise indicated.

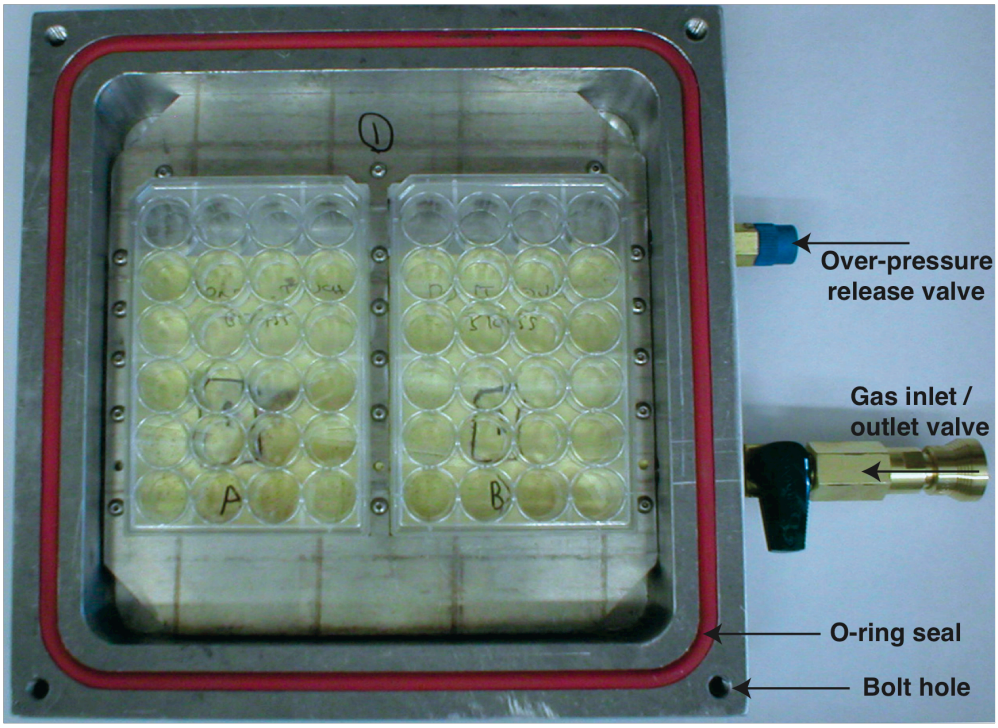


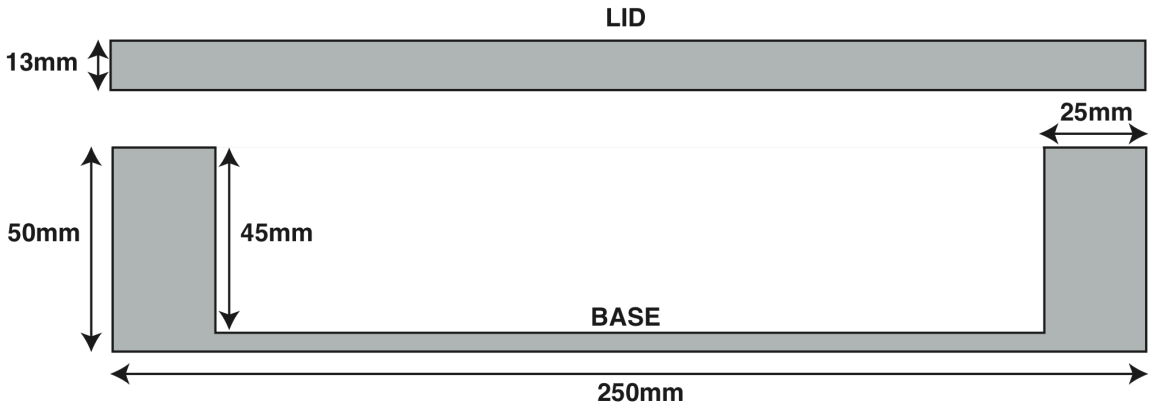


**Figure 3.1 Photograph and diagram of an aluminium hypoxia chamber**

A photograph of the hypoxia chamber (above) consisting of the aluminium base with gas inlet / outlet valve, overpressure release valve, o-ring seal, and bolt holes to allow the aluminium lid to be bolted in place. These aluminium chambers, designed and engineered by Dr. Andrew Minchinton and Dr. Alastair Kyle, allow for cell cultures to be rapidly rendered hypoxic and transported easily for administration of X-radiation. The aluminium bottom construction acts as a filter for the radiation beam to eliminate low energy photons as the radiation is delivered from below. Held within the chamber are two 24-well plates for housing the cell cultures that are to be irradiated. Below is a cross-section diagram of the hypoxia chamber with its dimensions.

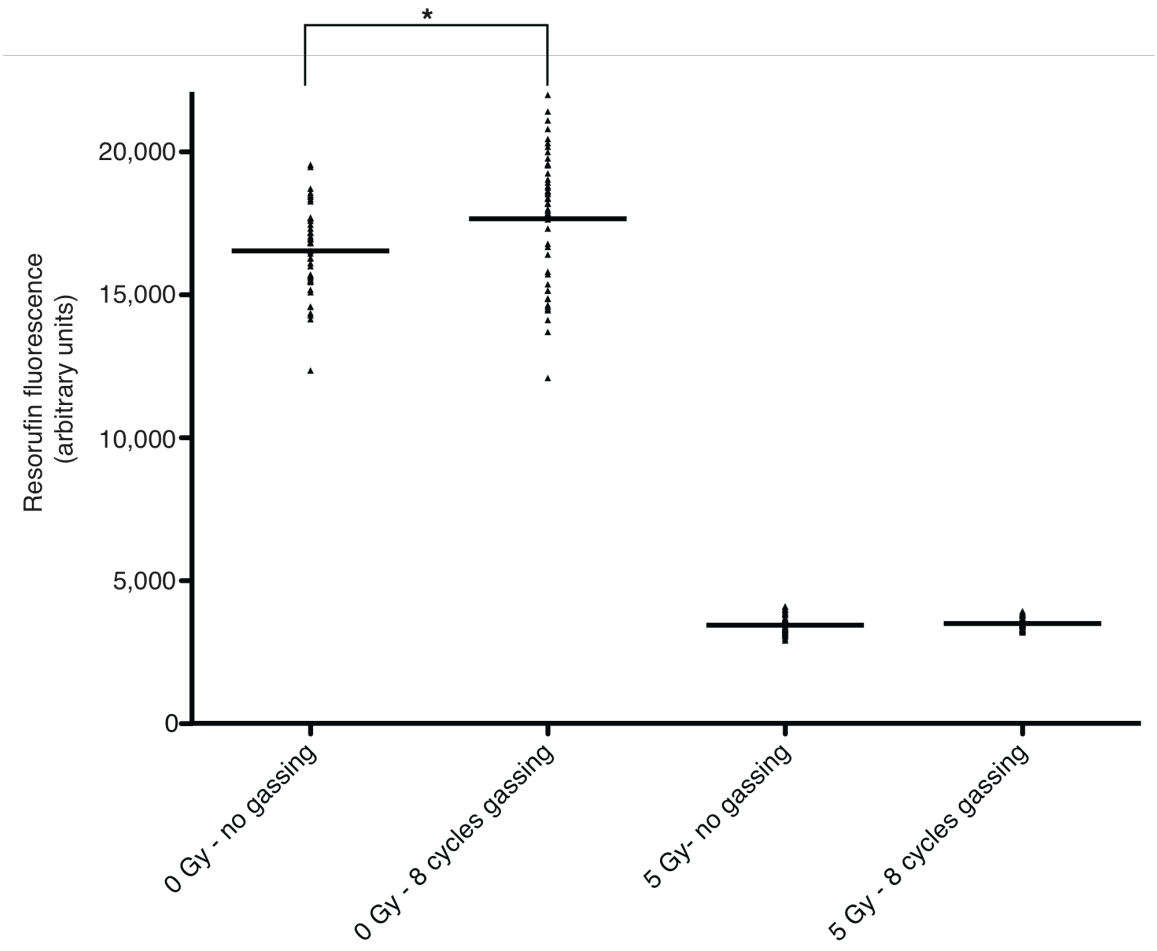


**Figure 3.2 Cell viability following gassing protocol with and without 5 Gy irradiation**
Cells treated with 8 cycles of gassing with 21% $O_2$/ 5% $CO_2$ / balance $N_2$, were compared to control cells treated with 10 min of atmospheric air. Following treatment cells were returned to normal incubation conditions for 72 h at which point the resazurin reduction assay was performed to assess cell viability. The graph above displays fluorescence readings from ≥ 40 replicate wells. Unexpectedly, the gassing protocol appears to cause a slight but significant increase in cell viability compared to the control cells ($P < 0.05$ student's unpaired, two tailed t-test). This difference is apparent in the non-irradiated (0 Gy) treatment group, but not in the irradiated (5 Gy) groups.

## 3.2 Hypoxia chamber development: the number of gas exchange cycles necessary to achieve maximum radiobiological hypoxia

### Introduction

Hypoxia can be defined as having a pO2 lower than normal, so a standard working definition of radiobiological hypoxia for the purpose of this thesis, is such that cells are rendered radiobiologically hypoxic if cell viability is greater in hypoxic cells following a given dose of radiation, compared to the viability of cells irradiated under conditions of ≥3% $O_2$. To further test the hypoxia chambers, the number of 30 s evacuation/ 30s pressurization gas exchange cycles in the hypoxia chamber necessary to achieve maximal radiobiological hypoxia was determined.

### Approach

The chamber was tested for its ability to render cells hypoxic by examining cell viability with the resazurin reduction assay, see section 2.4 for details. Briefly, cell viability was assessed 72 h following a gas exchange procedure consisting of 0-10 gas exchange cycles. Following gassing, cells were irradiated with 5 Gy. A control treatment representing 100% cell viability was included in which cells were neither gassed nor irradiated. As per the definition of radiobiological hypoxia, it is expected that if cells are being rendered hypoxic, their survival will increase following ionizing radiation treatment until a maximum level of radioresistance imparted by the hypoxia is reached, at which point cells are effectively anoxic. Prism GraphPad software for Macintosh V5.0b was used to fit these data to a variable slope sigmoidal dose-response curve.

### Results

The results of this experiment are displayed in figure 3.3. Following increased numbers of gassing cycles, cells became increasingly resistant to the effects of ionizing

radiation as displayed by the corresponding increase in cell viability. This increase in cell viability occurred up to ten gas exchange cycles. A protocol using eight gas exchange cycles was used throughout this work because it achieves a level of hypoxia that is close to, albeit slightly decreased from complete anoxia, which has been shown to induce cellular apoptosis (47). Although this level of hypoxia is sufficient for the purposes of this prodrug screening program, which requires only that cells display practical radiobiological hypoxia, future work could address more specifically the oxygen tensions achievable using this system. In order to specifically determine the level of dissolved oxygen within the cell cultures, an aluminium chamber will need to be modified to include an oxygen sensor that is in contact with the cell culture media. This likely could be achieved using a fibre optic oxygen sensor enclosed within the chamber through a sealed port.

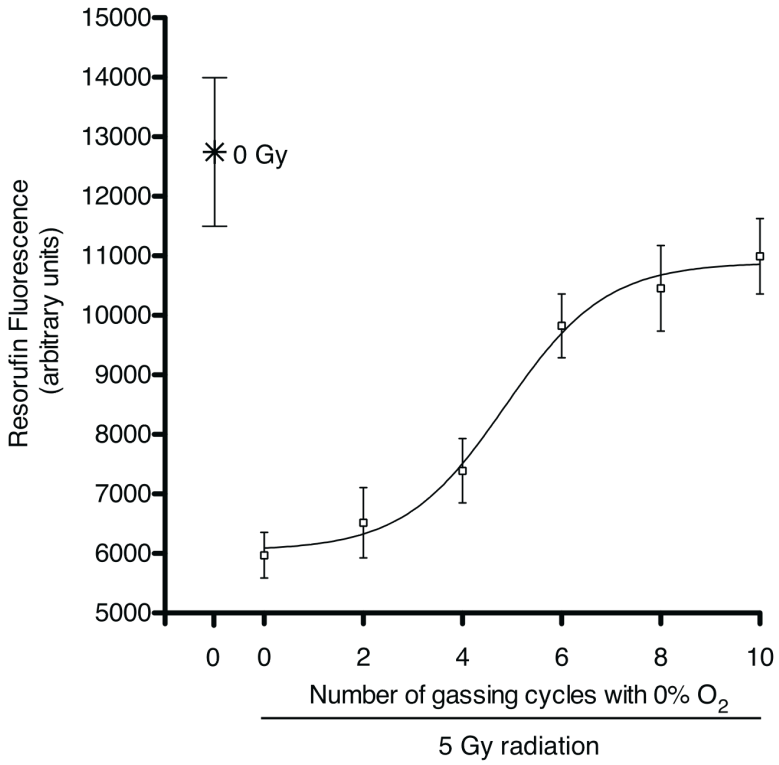


**Figure 3.3 HeLa cell viability following 2-10 cycles of gas exchange in hypoxia chambers and 5 Gy ionizing radiation.**

Each □ symbol represents an individual well from a 24-well plate that was placed within the hypoxia chamber and subject to the indicated number of gas exchange cycles prior to exposure to 5 Gy, with the exception of the 0 Gy non-irradiated contol. The dashed line represents the mean percent cell viability with respect to the non-irradiated control cells. After just two gas exchange cycles the cells display radiobiological hypoxia. Increasing the number of gas exchange cycles that replace the chamber air with a 0% $O_2$/ 5% $CO_2$/ balance $N_2$ gas mixture increases cell viability following exposure to 5 Gy ionizing radiation, indicating that the cells within the chamber have become radiobiologically hypoxic.

## 3.3 Hypoxia chamber development: differentiation between $pO_2$ tensions achieved using the hypoxia chambers

### Introduction

To further characterize the hypoxia chambers and assess the ability of the resazurin reduction assay to differentiate between levels of cell viability following radiation, we employed the resazurin reduction assay following gas exchange with various gases containing between 0-5% $O_2$ to induce different levels of hypoxia in combination with radiation dose response.

### Approach

To test for the ability to differentiate between differences in oxygen tension, CB.17 MEF cells plated on glass inserts within 24 well plates were placed within the hypoxia chamber on the multi-attenuator insert, described in section 3.4. The chambers were sealed and gassed with 5% $CO_2$/ balance $N_2$ gas mixtures containing 0%, 0.2%, 0.5%, and 5% oxygen before being irradiated. Following irradiation cells were removed from the chambers and returned to normal incubation conditions where they were allowed to recover for 72 h before being assayed for viability with the resazurin reduction assay; see section 2.4 for assay details.

### Results

The results presented **in** figure 3.4 demonstrate that cell viability was found to decrease along with oxygen tension at each of the radiation dose administered. Although statistical significance was not achieved between the various oxygen tensions at a given radiation dose, the trend of increasing radioresistance along with decreasing oxygen tension is consistent with the known radiation response to hypoxia, indicating that the chambers are functioning consistently in the gas exchange protocol and that the

resazurin reduction assay is sensitive enough to detect relatively small changes in cell viability.

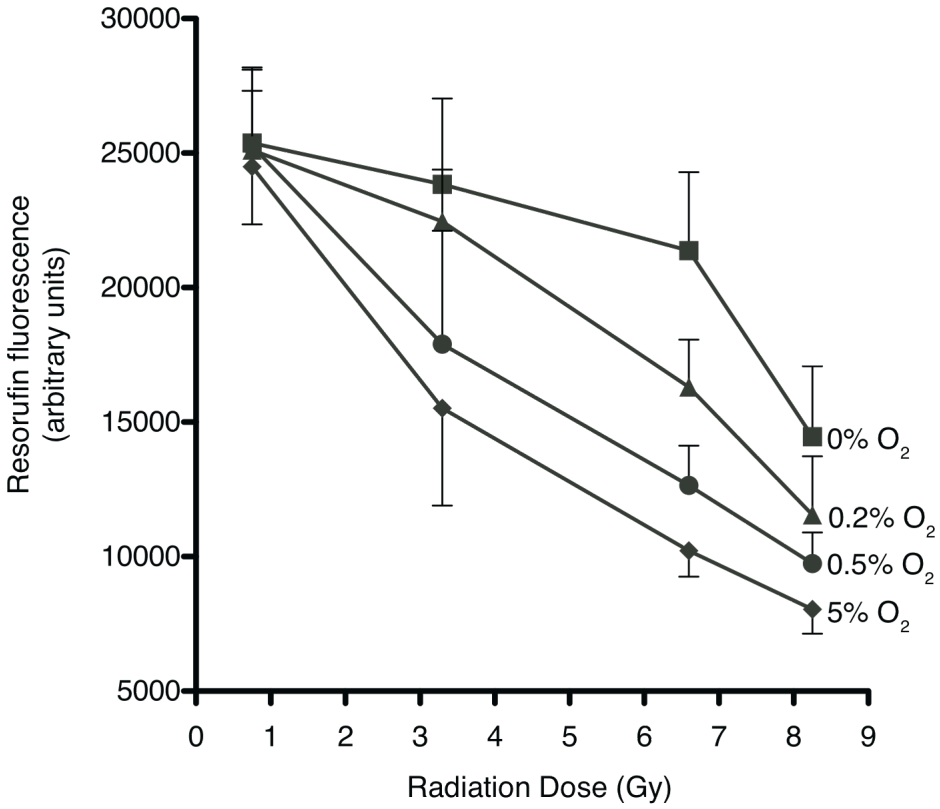


**Figure 3.4 Percent viability of CB.17 cells equilibrated to various levels of hypoxia in response to IR.**
This graph displays the results of a resazurin reduction assay in which CB.17 cells have been equilibrated to 0, 0.2, 0.5, or 5% $O_2$ conditions before exposure to various doses of ionizing radiation. With eight gas exchange cycles, cell viability is found to increase with decreasing oxygen tensions at all radiation doses. Although statistical significance is not achieved in viability differences between the various oxygen tensions, a clear trend displaying the radioprotectent effect of hypoxia is visible. Error bars represent the mean ± standard deviation for 7-8 wells of a 24 well plate.

## 3.4 Testing of a multi-attenuator insert to achieve multiple radiation doses with a single administration

### Introduction

In order to increase the throughput of the candidate compound screening assays, a multi-attenuator insert was designed and built by Dr. Alastair Kyle. This insert was tested for radiation dosimetry and compatibility with the resazurin reduction assay by the author in concert with Dr. Kyle. The multi-attenuator insert fits within the hypoxia chamber, housing two 24-well plates, functioning to attenuate the intensity of the radiation beam across the plates. It is designed such that each of six columns in the 24 well plates receives different radiation doses when a single radiation administration is delivered from below, see figure 3.5, left. The ability to achieve multiple radiation doses with a single administration drastically shortens the time required to perform experiments assessing the effect of candidate prodrugs across various doses of radiation.

### Approach

The amount of attenuation achieved across each column was determined using thermoluminescent dosimetry (TLD). TLD chips were placed within the wells of a 24-well plate containing glass inserts, corresponding to where cells would be in a typical experimental set up for either the clonogenic or resazurin reduction assays. A control chip that remained outside of the chamber was included to determine a background radiation reading. The background TLD value was subtracted from all readings and values were normalized to column 1 which contains no attenuating material and was designated as 0% attenuation.

To visualize the attenuation, a piece of X-ray film was placed over top of the multi-attenuator and sealed within the chamber in a dark room. The chamber was then

irradiated with the equivalent of 3 Gy before the film was removed in the darkroom and developed.

**Results**

The results of the TLD measurments are displayed in Table 3-1. The attenuation was also visualized using X-ray film placed within the chamber prior to radiation delivery, see figure 3.5, right.

**Table 3-1 A list of the attenuating agents used to make the multi-attenuator and corresponding percent attenuation**

| 24 well plate column | Attenuating agent | Background subtracted TLD reading (arbitrary units) | Percent attenuation of administered dose |
|---|---|---|---|
| 1 | None | 8073 | 0% |
| 2 | 0.25 mm brass | 6089 | 25% |
| 3 | 0.76 mm brass | 4513 | 44% |
| 4 | 1.52 mm brass | 3614 | 55% |
| 5 | 1.52 mm brass, 0.38 mm lead | 1867 | 77% |
| 6 | 1.52 mm brass, 11.38mm lead | 436 | 95% |

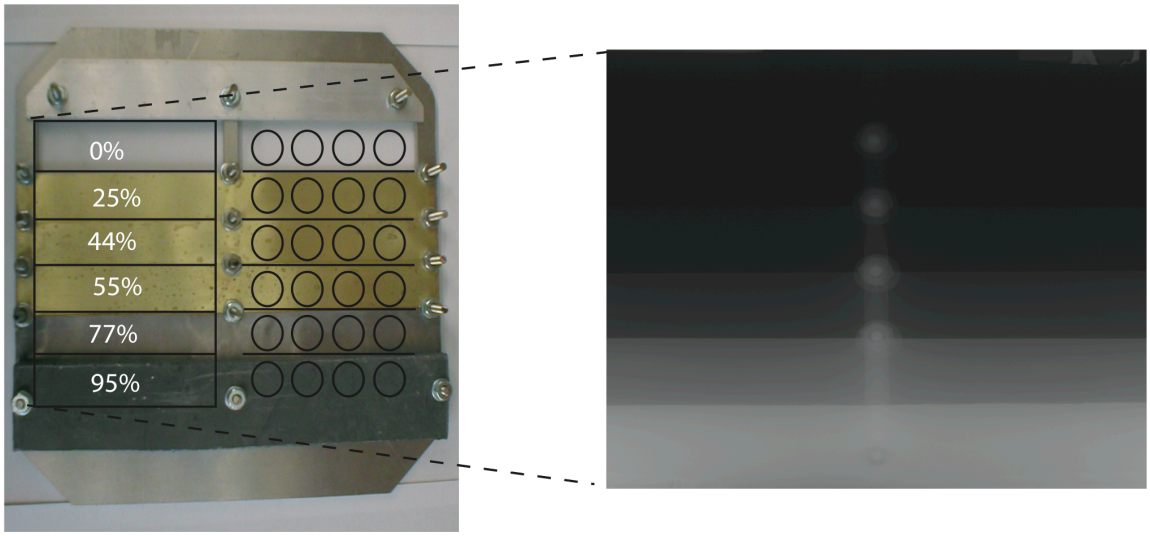


**Figure 3.5 Photograph and X-ray film of the multi-attenuator insert.**

This multi-attenuator insert made from stainless steel, brass and lead, fits within the hypoxia chamber and functions to attenuate the radiation beam across the six columns of two 24-well plates, such that a gradient of radiation doses is achieved during one delivery of radiation. Left, a photograph of the underside of the multi-attenuator insert with an overlay displaying the percentage of attenuation achieved across each column (white text) and the placement of the wells in a 24-well plate (black circles). Right, an x-ray film that was placed within the sealed hypoxia chamber containing the multi-attenuator insert prior to delivering 3.5 Gy displays the gradient of radiation exposure received across the insert.

# Chapter 4: Establishment of proof of principle

A number of studies have demonstrated the radiosensitizing ability of broadly selective PI3K and PIKK inhibitors such as wortmannin and LY294002 as well as inhibitors that are more selective to DNA-PK such as PI-103, NU7441, IC87361 in oxic cells, see Appendix B. However, very few studies have been published exploring the inhibition of DNA-PK in *hypoxic* cells, and thereby it was necessary to establish that inhibition of DNA-PK in hypoxic cancer cells would sensitize hypoxic cells to ionizing radiation. This chapter includes experimental evidence that all three subunits of DNA-PK are expressed in hypoxic cells, and that genetic inactivation and chemical inhibition of DNA-PK can radiosensitize hypoxic mouse embryonic fibroblast (MEF) and human cervical carcinoma cells. Also included is a proof of principle experiment surrounding the design of hypoxia activated prodrugs of the DNA-PK inhibitor IC86621, referred to as HAPI2 and HAPI3.

## 4.1 DNA-PKcs, Ku70, and Ku80 protein expression is stable in HeLa human cervical cancer cells under hypoxic conditions

### Introduction

The expression of key proteins within the HRR pathway, including Rad51, Rad54, and XRCC3 has been shown by Chan et al. to decrease under conditions of chronic hypoxia, affecting the function of HRR in hypoxic cells (9). It is well established that a number of cellular processes are altered in response to hypoxic stress, and arguably the most characterized mediator of these processes is a transcription factor protein called hypoxia inducible factor 1 alpha (HIF1-$\alpha$). In the presence of molecular

oxygen HIF1-α is hydroxylated at two critical proline residues by prolyl hydroxylase (PHD) enzymes (48). This hydroxylation targets HIF1-α for proteasomal degradation. However, in hypoxic conditions HIF1-α expression is stabilized, resulting in HIF1-α mediated gene expression changes which affect various cellular processes such as energy metabolism, proliferation, apoptosis, and angiogenesis (48).

In order for the proposed prodrugs to be effective it is crucially important for the target protein, DNA-PK, to be expressed in hypoxic cells. There are only a small number of reports investigating the expression of either protein or mRNA expression for DNA-PK under hypoxic conditions (49, 50). Therefore, in order to confirm the presence of the drug target we have assessed the protein expression level of the three DNA-PK subunits, DNA-PKcs, ku70, and ku80, in acute and chronically hypoxic HeLa cells.

**Approach**

Details of this protocol are presented in section 2.9. Briefly, HeLa cells were grown in a humidified 37 °C incubator within a 1% $O_2$/ 5% $CO_2$ glove box. At time points between 4-72 h cells were lysed. Whole cell lysate was separated by SDS-PAGE, transferred to 0.45 μm pore size nitrocellulose membrane and probed with antibodies against Ku70, Ku80, DNA-PKcs, HIF1-α, and β-tubulin. Secondary antibodies were HRP conjugated and enhanced chemiluminescence was carried out with film detection. Densitometry was performed on digital images of scanned films using NIH ImageJ V1.42 for Macintosh.

**Results**

Figure 4.1 presents the protein expression of each of the DNA-PK components from HeLa cell whole cell lysate collected following exposure to 1% oxygen for 4, 24, 48, and 72 h; β-tubulin is included as a protein loading control. Also displayed is the HIF1-α

expression, which was found to increase with time under hypoxia up to 72 h, at which point HIF1-$\alpha$ expression decreased. This decrease in HIF1-$\alpha$ expression is consistent with the up-regulation of PHD enzymes, which de-stabilize HIF1-$\alpha$ following prolonged exposure to hypoxia (51). Expression of DNA-PKcs was found to be relatively stable throughout hypoxia, however there is an increase in both Ku70 and Ku80 expression visible after 4 h and peaking after 48 h, and with levels remaining higher than in oxic cells after 72h. This result confirms a strong presence of DNA-PK in hypoxic cells, supporting its suitability as a target for hypoxia activated DNA repair inhibitors.

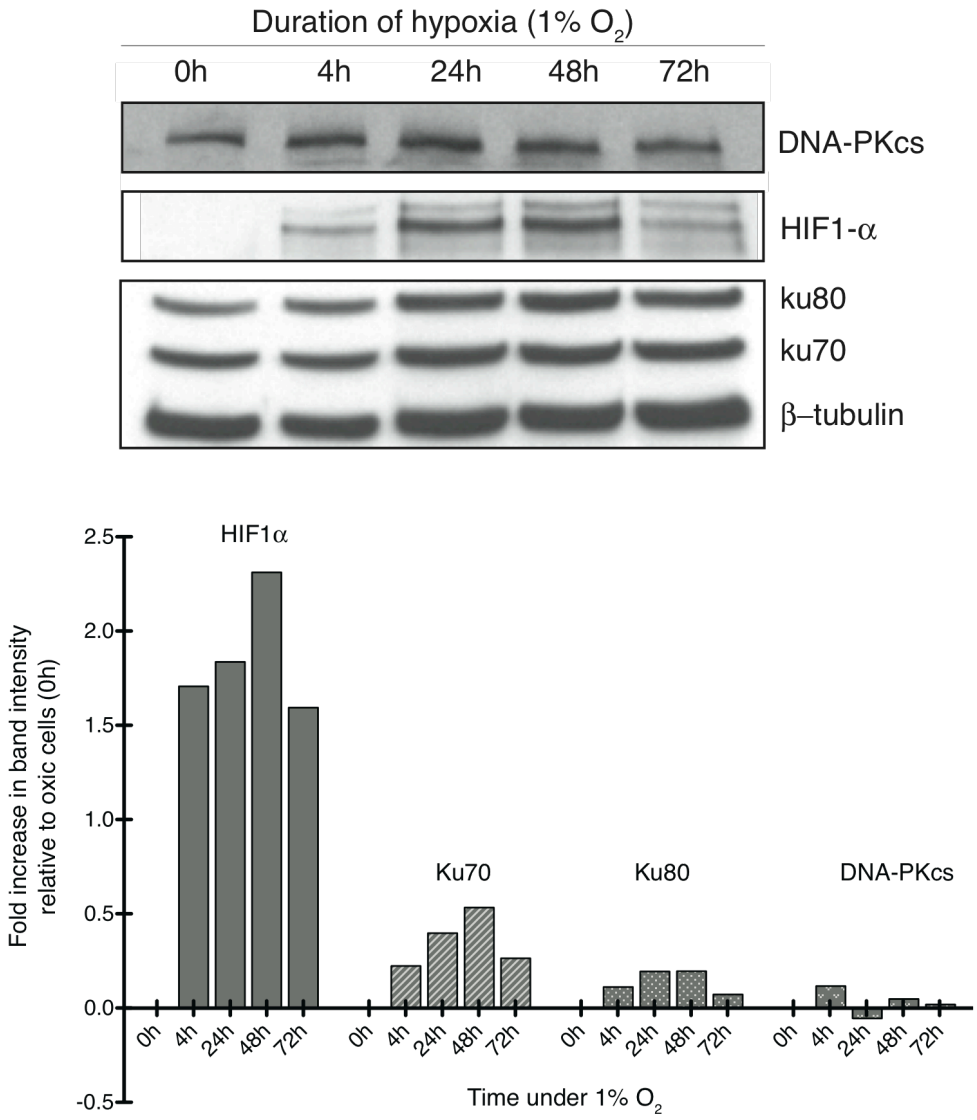


**Figure 4.1 HeLa cell protein expression of DNA dependent protein kinase subunits following 4-72 hours of hypoxia at 1% oxygen**

Displayed is a western blot analysis of the proetin expression for the three DNA-PK subunits, DNA-PKcs, Ku70, and Ku80, following exposure to hypoxic conditions (1% $O_2$/ 5% $CO_2$/ balance $N_2$) for 4-72 h. HIF1α is included as a hypoxia biomarker and β-tubulin is incuded as a loading control. Densitometry of the bands (normalized first to the β-tubulin loading control and secondly to the oxic cells) is displayed in the graph below.

The protein expression of DNA-PKcs is relatively stable in hypoxic conditions, however there is an increase in the expression of Ku70 and Ku80 visible by 4 h and peaking at 48 h under 1% oxygen. The strong protein expression of DNA-PKcs and the Ku subunits in hypoxic cells suggests that DNA-PK expression is greater under hypoxia and supports the selection of DNA-PK as a target for hypoxia activated DNA repair inhibitors.

## 4.2 Genetic DNA-PK deficiency causes sensitivity to ionizing radiation independent of hypoxia

### Introduction

Previous work with DNA-PK inhibitors has shown their ability to sensitize cancer cells in culture and human xenograft tumours in mice to the effects of DNA damaging agents under normoxic conditions, however, the effects of DNA-PK inhibitors on the sensitivity of hypoxic cells to ionizing radiation has not yet been thoroughly explored (52-54). In one study by He et al., adenoviral mediated expression of a dominant negative Ku70 variant was shown to radiosensitize hypoxic human glioma and colorectal carcinoma cells that were equilibrated to 0.5% $O_2$ for 24 h prior to irradiation (55). A second study by Murray et al. has examined the effects of oxygen on the radiosensitivity of two human glioma cell lines derived from the same tumour, one of which expresses functional DNA-PKcs, called M059K, and the other which lacks functional DNA-PKcs, M059J. This study demonstrated that DNA-PKcs deficient M059J cells are hypersensitive to ionizing radiation compared to DNA-PKcs wild-type M059K cells, *independent of hypoxia* (6). Both of these results support the proposal that inhibition of DNA-PK activity would sensitize mammalian cells to the cell killing effects of ionizing radiation independent of the presence of molecular oxygen.

To further assess the effect of DNA-PK inhibition on cellular radiosensitivity in hypoxic conditions, we took advantage of two mouse embryonic fibroblast (MEF) cell lines that were originally derived from the CB.17 mouse strain, however one of which is from a mouse harbouring the naturally occurring SCID mutation (56). The SCID mutation codes for a nonsense mutation at tyrosine 4046 in both copies of the *prkdc* gene, resulting in low level transcription of a c-terminal truncated form of the DNA-PKcs protein, which lacks the kinase domain required for DNA-PK dependent NHEJ activity

(57). The degree to which cell survival is affected following IR is relative to the extent of hypoxia within the cultures, and is commonly expressed by the oxygen enhancement ratio (OER) as mentioned previously.

**Approach**

Details of the clonogenic survival assay are described in section 2.5. Briefly, DNA-PK deficient cells, SCID/st, and DNA-PK wild-type cells, CB.17, were plated into glass petri dishes and allowed to adhere overnight. The next day cells were gassed and irradiated under oxic (21% $O_2$/ 5% $CO_2$/ balance $N_2$) and hypoxic conditions (0% $O_2$/ 5% $CO_2$/ balance $N_2$) using the aluminium chambers described in section 3.2. Immediately following irradiation, cells were removed from the chambers, harvested by trypsinization, and re-plated on round tissue culture dishes at dilutions predicted to yield 100 colonies. Plates were left undisturbed under standard incubation conditions for two weeks before the medium was removed and colonies of cells were stained purple with crystal violet and counted.

**Results**

MEF cells derived from a wild type CB.17 mouse were irradiated following equilibration to atmospheric oxygen conditions (21% $O_2$) or hypoxic conditions (0% $O_2$). As anticipated from previous studies, the surviving fraction of CB.17 cells was increased when radiation was administered under hypoxic conditions, producing an OER of ~2.6, see figure 4.2 red circles. MEF cells derived from a CB.17 mouse harbouring the SCID defect, SCID/st, were similarly irradiated and assessed for clonogenic survival. As with the DNA-PKcs proficient CB.17 cells, SCID/st cells lacking functional DNA-PK activity display enhanced clonogenic survival following irradiation under hypoxic conditions, resulting in an OER of ~2.4, see figure 4.2 black triangles. Notably, the hypoxic DNA-

PKcs deficient SCID/st cells are similar in radiosensitivity to oxygenated DNA-PKcs proficient CB.17 cells.

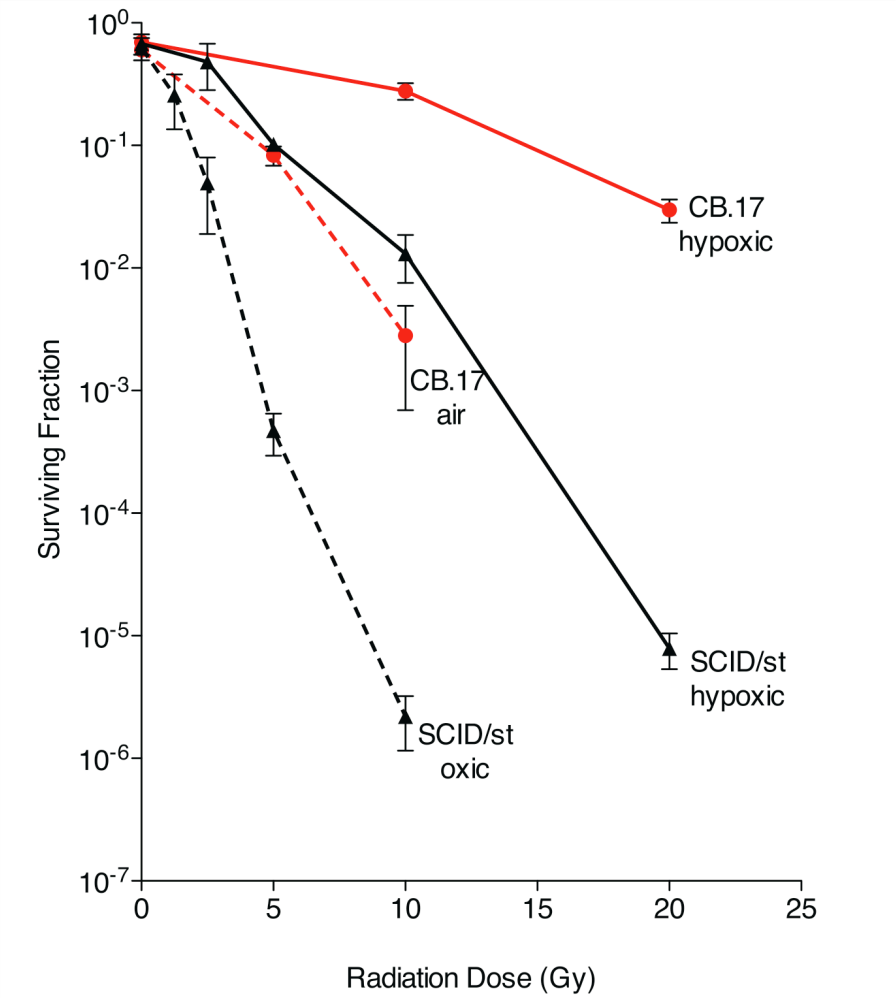


**Figure 4.2 The survival of oxic and hypoxic CB.17 and SCID/st cells following exposure to ionizing radiation**

The clonogenic survival of immortalized fibroblasts originally derived from a wild type CB.17 mouse (CB.17) and those from a mouse harbouring the SCID defect (SCID/st) was assessed following administration of ionizing radiation under either 21%$O_2$ or 0% $O_2$. The SCID defect is caused by a homozygous nonsense mutation in the *prkdc* gene, which results in a DNA-PK deficiency. Consistant with previous studies, SCID/st cells display radiation hypersensitivity when irradiated in 21% $O_2$, however under hypoxic conditions, SCID/st cells remain radiosensitive when compared to hypoxic CB.17 cells similarly irradiated. This result indicates that DNA-PK deficent cells are hypersensitive to ionizing radiaiton independent of the presence of molecular oxygen at the time of irradiation.

## 4.3 Chemical inhibition of DNA-PK can sensitize both oxic and hypoxic cells to the effects of ionizing radiation

### Introduction

As we are interested in chemically inhibiting DNA-PK selectively in hypoxic cells, it is necessary that chemical inhibitors of DNA-PK can act to sensitize hypoxic cells to radiation in a manner similar to that displayed by genetic deficiency. To assess the affects of chemical inhibition on the radiosensitivity of hypoxic cells we treated CB.17 cells with the DNA-PK inhibitors IC86621 and NU7026 either alone or in combination with radiation under oxic and hypoxic conditions. These two compounds were chosen for their selectivity against DNA-PK as well as the availability of published preclinical data regarding their efficiency at radiosensitizing oxic cells (31, 58). We were particularly interested in IC86621 due to its chemical structure, which has a 2-hydroxyl group that is particularly amenable for conjugation to a hypoxia activated trigger. For the chemical structures and published $IC_{50}$ values of the individual inhibitors see Appendices A and B.

As the graph of radiation induced DSB repair versus time displays a biphasic exponential curve, it is widely accepted that DSB repair consists of both a fast and slow repair component (59). The reported half lives of DSB repair for each of these components is on the order of 5-15 min for fast repair, which is thought to occur for simple or clean breaks that are easily repaired by the cell, and 1-15 h for the slower component of repair of more complex breaks (59-61). Because the fast component of DSB repair can occur very quickly, an anti-cancer agent that inhibits DSB repair must be administered prior to the delivery of the DNA damaging agent in order for it to be maximally effective. In the case of hypoxia activated prodrugs, administration of the prodrug to patients would need to occur prior to administration of radiation therapy.

Thus, in experiments involving DNA-PK inhibitors and radiation we have pre-treated cells with the DNA-PK inhibitor prior to the administration of IR.

**Approach**

In these experiments, CB.17 cells were pre-treated for 1h with DNA-PK inhibitors or an equivalent amount of DMSO as a vehicle control; 1% DMSO for 30 μM NU7026 and 0.1% DMSO for 100 μM IC86621. Following the pre-treatment period, cells were equilibrated to hypoxic conditions (0% $O_2$/ 5% $CO_2$/ balance $N_2$) or oxic conditions (21% $O_2$/ 5% $CO_2$/ balance $N_2$) and subsequently irradiated using our aluminum chambers containing the multi-attenuator insert described in section 3.4. The DNA-PK inhibitor or DMSO (vehicle control) remained on the cells for 24 h following administration of IR. Cells were then allowed to recover for an additional 48 h in the absence of DNA-PK inhibitor or DMSO before cell viability was assessed by the addition of resazurin dye (refer to section 2.4 for details of this assay). The values reported are the mean ± standard error of the mean for at least three intra-experiment replicates. Percent viability was determined by normalizing fluorescent values such that the non-irradiated control in each treatment group represents 100% viability and background fluorescence represents 0% viability.

**Results**

Figure 4.3 displays the results of a cell viability assay performed after treating both oxic and hypoxic CB.17 cells with the DNA-PK inhibitor IC86621 in combination with various radiation doses. Oxic and hypoxic CB.17 cells were sensitized to the effects of IR when treated with the DNA-PK inhibitor. Both 50 and 100 μM IC86621 were able to sensitize hypoxic CB.17 cells to the effects of ionizing radiation, and did so in a dose dependent manner.

Similarly, the more selective DNA-PK inhibitor NU7026 also radiosensitized both oxic and hypoxic CB.17 cells, as displayed in figure 4.4. Here, hypoxic CB.17 cells treated with 30 μM NU7026 were sensitized to the effects of IR. It is important to note that the radiosensitization effect observed with the use of DNA-PK inhibitors occurs at clinically relevant doses of administered radiation, which is normally delivered in fractions of 2-3 Gy.

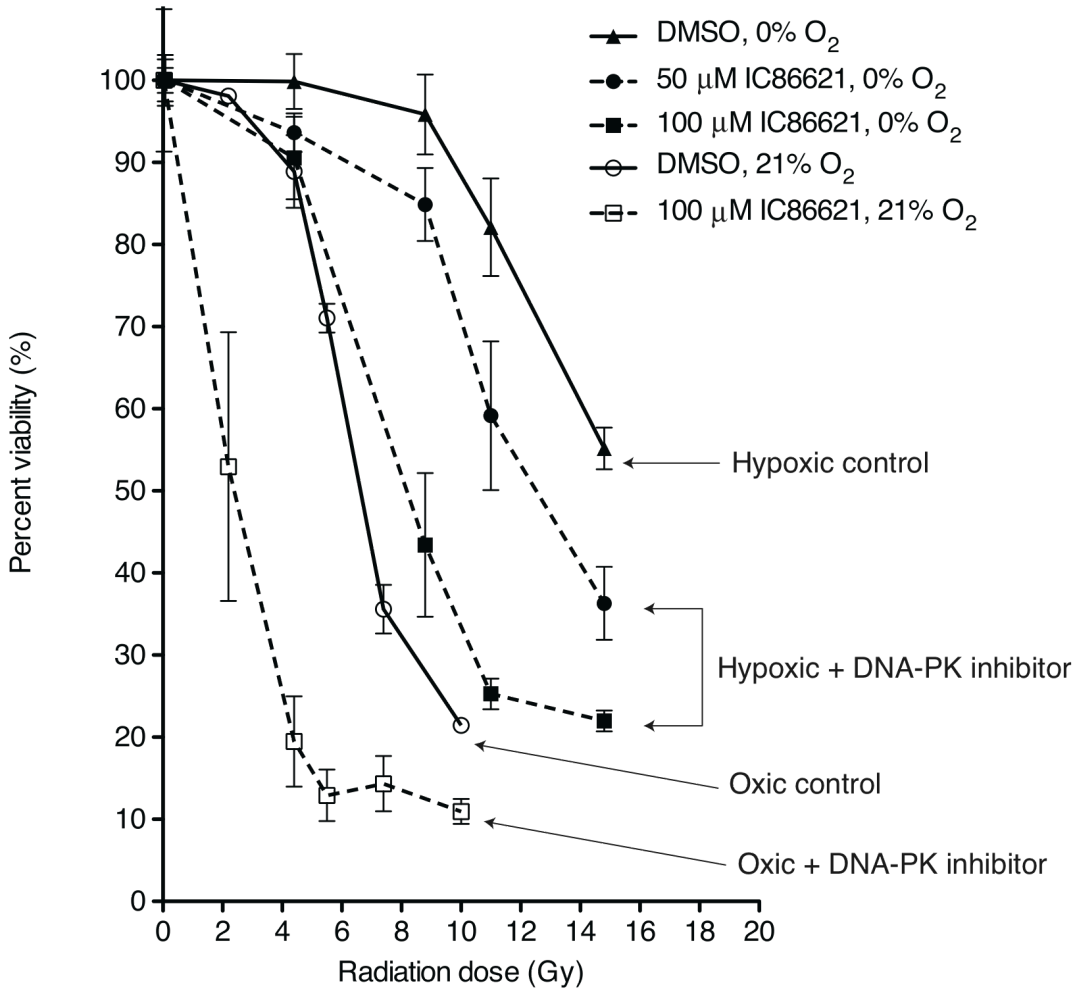


**Figure 4.3 Radiosensitization of oxic and hypoxic CB.17 cells by IC86621**

CB.17 cells were pre-treated with 50 or 100 μM IC86621 or 0.1% DMSO as a vehicle control. Cells were equilibrated to oxic conditions (21% $O_2$/ 5% $CO_2$/ balance $N_2$) or hypoxia (0% $O_2$/ 5% $CO_2$/ balance $N_2$) before being irradiated at various doses. Viability was assessed using the resazurin reduction assay.

Hypoxic CB.17 cells are sensitized to radiation by the DNA-PK inhibitor IC86621 in a manner that is dependent on the dose of IC86621 (50 μM ● and 100 μM ■). Additionally, both oxic and hypoxic cells treated with IC86621 (dashed lines) are radiosensitive compared to the respective controls (solid lines). These findings demonstrate that CB.17 cells can be sensitized to the effects of ionizing radiation in an oxygen dependent manner by inhibiting DNA-PK. This supports the design of hypoxia activated prodrugs targeting DNA-PK by displaying the potential efficacy of the effector component of the prodrug in hypoxic conditions. Data points represent the mean ± standard error of the mean of at least three intraexperiment replicates.

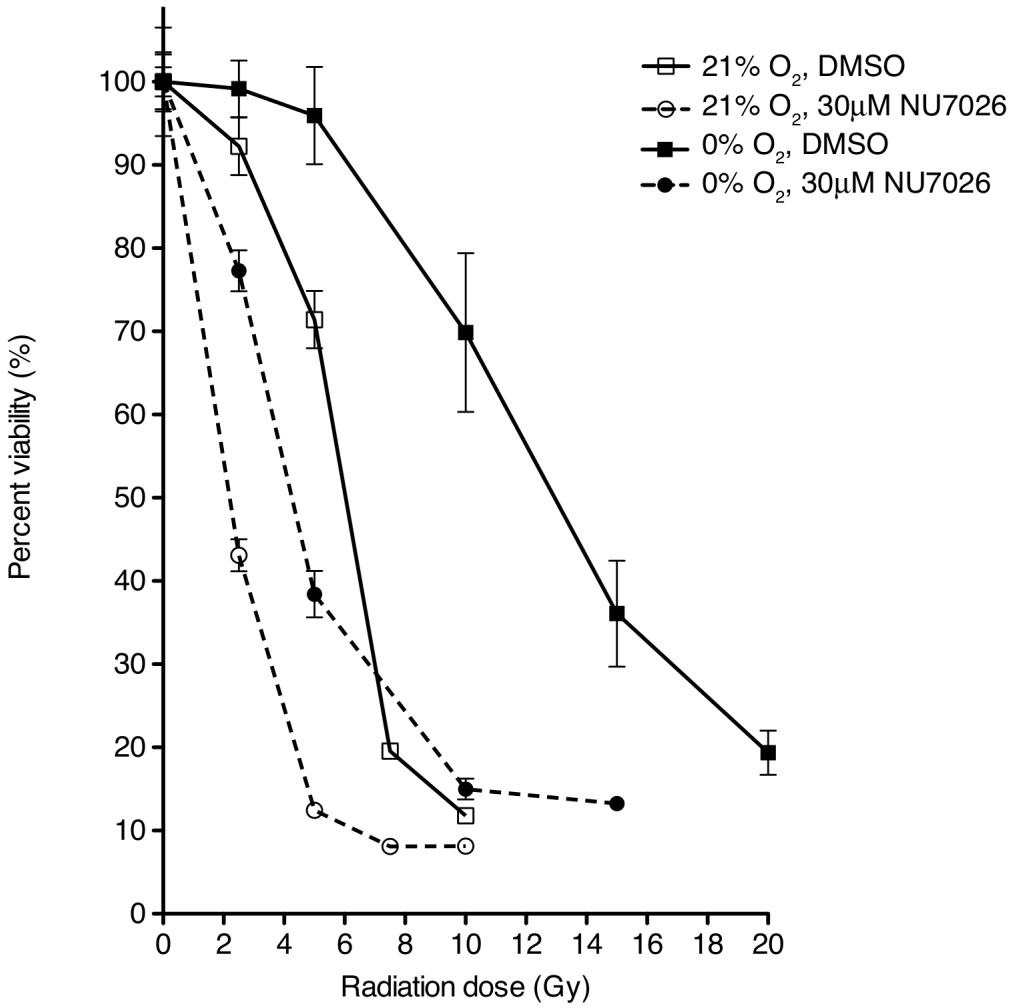


**Figure 4.4 Radiosensitization of oxic and hypoxic CB.17 cells by NU7026**

CB.17 cells were pre-treated with 30 μM NU7026 or 1% DMSO as a vehicle control and were equilibrated to oxic conditions (21% $O_2$/ 5% $CO_2$/ balance $N_2$) or hypoxia (0% $O_2$/ 5% $CO_2$/ blance $N_2$) before being irradiated. Viability was assessed using the resazurin reduction assay.

The results display that 30 μM NU7026 (dashed lines) for 1 h before and 24 h following ionizing radiation treatment can radiosensitize both oxic (open symbols) and hypoxic (closed symbols) CB.17 cells compared to vehicle treated controls (1% DMSO, solid lines). Points represent the mean ± SEM for of at least three intraexperiment replicates.

## 4.4 Residual DNA damage is increased in cells when treated with the DNA-PK inhibitor IC86621 in combination with ionizing radiation

### Introduction

Among the numerous post-translational modifications known to occur on histone proteins is the phosphorylation of serine residue 139 on histone H2A.X. When phosphorylated at serine 139, H2A.X is termed γH2AX. H2A.X is a variant of the minor histone protein, H2A. Phosphorylation of H2A.X generally occurs rapidly in large kilobase regions of chromatin surrounding newly generated DNA DSB, and is thought to act as an amplification signal to recruit proteins involved in the DNA damage response(62). Foci of γH2AX can be identified in the nuclei of cells containing DSB by using antibodies generated against serine 139 phosphorylated H2A.X. Analysis of cellular γH2AX levels by immunofluorescence, using either microscopy or flow cytometry, is a well-described method used to monitor the generation and repair of DSB, through the formation and resolution of γH2AX foci respectively (63, 64). The primary kinase responsible for phosphorylating H2A.X at serine 139 in response to DNA damage is ATM. However DNA-PK has been shown to contribute to γH2AX formation and acts redundantly in cells where ATM is deficient (62, 65, 66). As cell cycle checkpoint activation tends to occur in cells with extensive DNA damage, we have also analyzed the distribution of cells throughout the cell cycle by assessing DNA content (67).

### Approach

Following treatment with hypoxia, DNA-PK inhibitor IC86621, and IR, we have used flow cytometry to analyze cellular levels of γH2AX as a marker of DSB and have assessed cell cycle distribution using the DNA binding dye, 4',6-diamidino-2-phenylindole (DAPI). Flow cytometry and cell cycle analysis was performed by Dr.

Robyn Seipp as outlined in section 2.6. Briefly, HeLa cells plated on 60 mm diameter glass petri dishes were pre-treated for 1 h with either the DNA-PK inhibitor IC86621, or DMSO as a vehicle control and were gassed immediately following drug administration. Cell cultures were gassed and irradiated according to the method outlined in section 2.1. The gassing occurred 1 h prior to irradiation and cells were released from the hypoxia chamber to normal incubation conditions 1 h following irradiation. IC86621 or DMSO treatment continued following the administration of radiation until cells were collected and fixed with cold methanol 1 h or 24 h following irradiation. In these experiments HeLa human cervical carcinoma cells were used because they provide a more relevant model for human cancer than the CB.17 MEF cell line. The hypoxic conditions used in these experiments represent cells treated with 0.2% $O_2$/ 5% $CO_2$/ balance $N_2$ while the oxic conditions represent cells treated with the equivalent of atmospheric air, 21% $O_2$/ 5% $CO_2$/ balance $N_2$.

**Results**

DNA-PK inhibition resulted in higher γH2AX levels 24 h after irradiation, see figure 4.5 A**.** The increase in γH2AX levels 24 h after irradiation is indicative of increased residual DNA damage in the DNA-PK inhibitor treated cells, relative to vehicle treated controls. This effect was found to be independent of the dose of radiation to which cells were subjected, as at both 2.5 Gy and 5 Gy irradiation γH2AX levels are increased in the DNA-PK inhibitor treated cells relative to vehicle treated controls irradiated at the same dose.

Similarly, this trend of increased γH2AX in IC86621 versus DMSO controls was found to be independent of the amount of oxygen present at the time of irradiation, as seen in figure 4.5 B. At all oxygen tensions measured, treatment with the DNA-PK inhibitor lead to increased γH2AX levels 24 h following irradiation relative to vehicle

treated controls. γH2AX levels were found to increase with increasing oxygen tension, indicating that increasing the $pO_2$ of cells results in increasing levels of DNA damage from IR. This result is consistent with the oxygen effect and the oxygen fixation hypothesis described in section 1.1. IC86621 did not affect the initial amount of γH2AX induced one hour following irradiation, or in non-irradiated control cells, see figure 4.5 C.

The increase in γH2AX levels with DNA-PK inhibitor treatment controls was found to be dependent on the dose of IC86621 treatment in the 50-150 μM range, see figure 4.6 A. 24 h following 5 Gy irradiation under both oxic and hypoxic conditions, γH2AX increases along with the concentrations of IC86621 relative to the vehicle control. IC86621 treatment displays no obvious effects on γH2AX levels of non-irradiated control cells, outside of a minor increase in γH2AX in both oxic and hypoxic cells at the 150 μM treatment level.

In our analysis of cell cycle distribution we found that γH2AX levels correlated closely with increased numbers of cells in the G2 phase of the cell cycle following irradiation, see figure 4.6 B. Treatment with 100μM IC86621 increased the proportion of cells in the G2 phase of cell cycle relative to vehicle treated controls, while non-irradiated cells treated with IC86621 did not demonstrate large differences in cell cycle relative to controls, outside of a small increase in the G1 population of cells in IC86621-treated non-irradiated cells which was often observed. This increase in G1 cells may be due to off target effects of the IC86621 inhibitor, which is likely to also be inhibiting the PI3K signalling pathway through inhibition of P110β at the 100 μM treatment level, see appendix B for $IC_{50}$ values. Inhibition of PI3K signalling results in decreased phosphorylation of the signal transduction protein Akt, whose downstream targets are mediators of cell cycle entry (68).

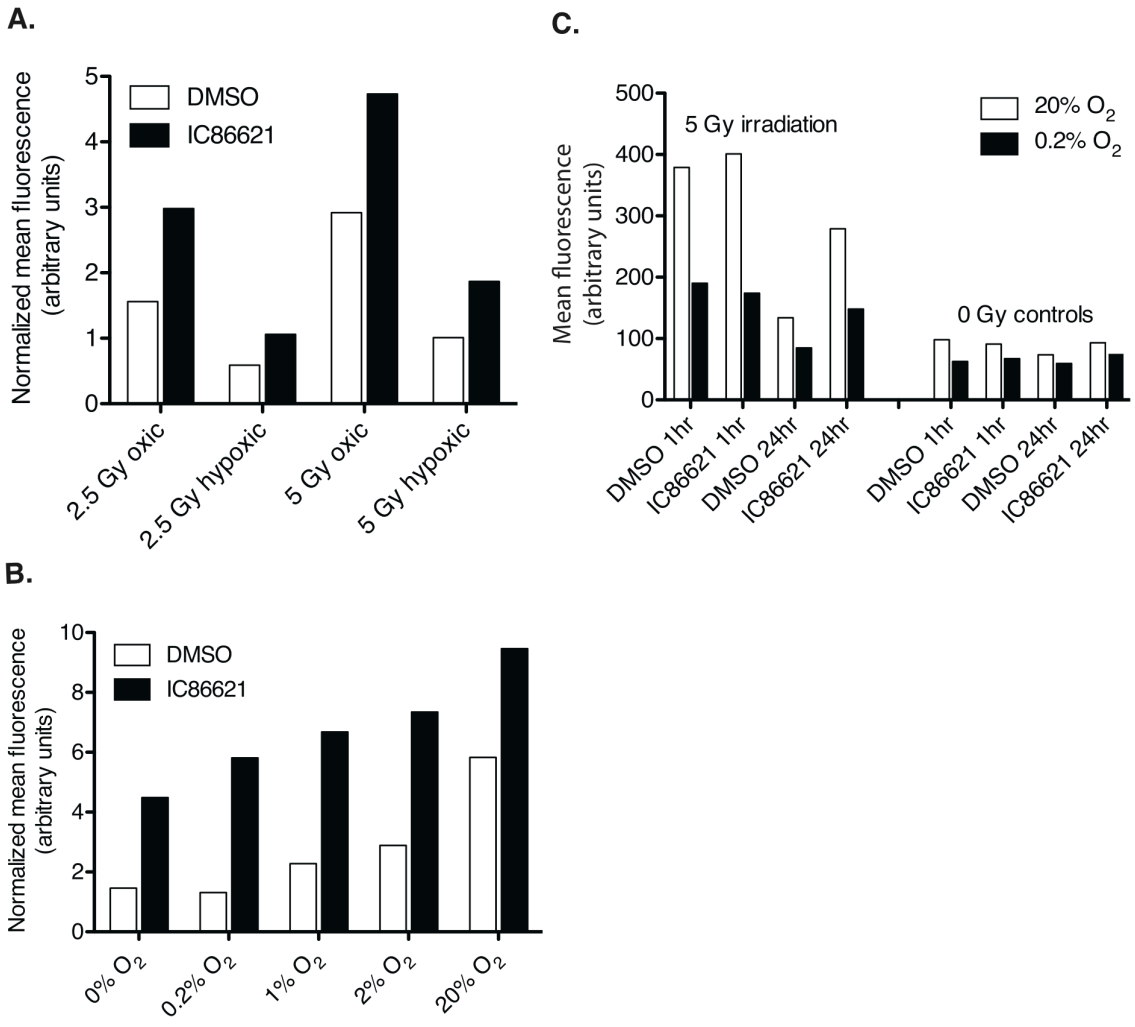


**Figure 4.5 DNA-PK inhibitor IC86621 increases residual DNA damage in HeLa cells 24h following treatment with ionizing radiation**

HeLa cells treated with 100 µM IC86621 or 0.1% DMSO as a vehicle control were equilibrated to various concentrations of oxygen (0-21% $O_2$/5% $CO_2$/ balance $N_2$) for 1h prior to irradiation. The mean γH2AX intensity of >10,000 cells was observed using flow cytometry.

A) γH2AX intensity increased with 100 µM IC86621 treatment in combination with IR doses of 2.5 and 5 Gy under both oxic and hypoxic conditions. B) γH2AX intensity increases along with oxygen concentration 24 h following 5 Gy IR with or without IC86621 treatment. At all oxygen concentrations tested, γH2AX intensity in IC86621 treated cells is greater than that of cells treated with the vehicle control DMSO. C) γH2AX intensity is unaffected by IC86621 1h following 5 Gy irradiation in oxic and hypoxic conditions, however 24h following IR γH2AX intensity is greater in IC86621 treated cells compared to vehicle treated controls. These results indicate that the DNA-PK inhibitor IC86621 functions to increase the amount of residual DNA damage remaining in cells

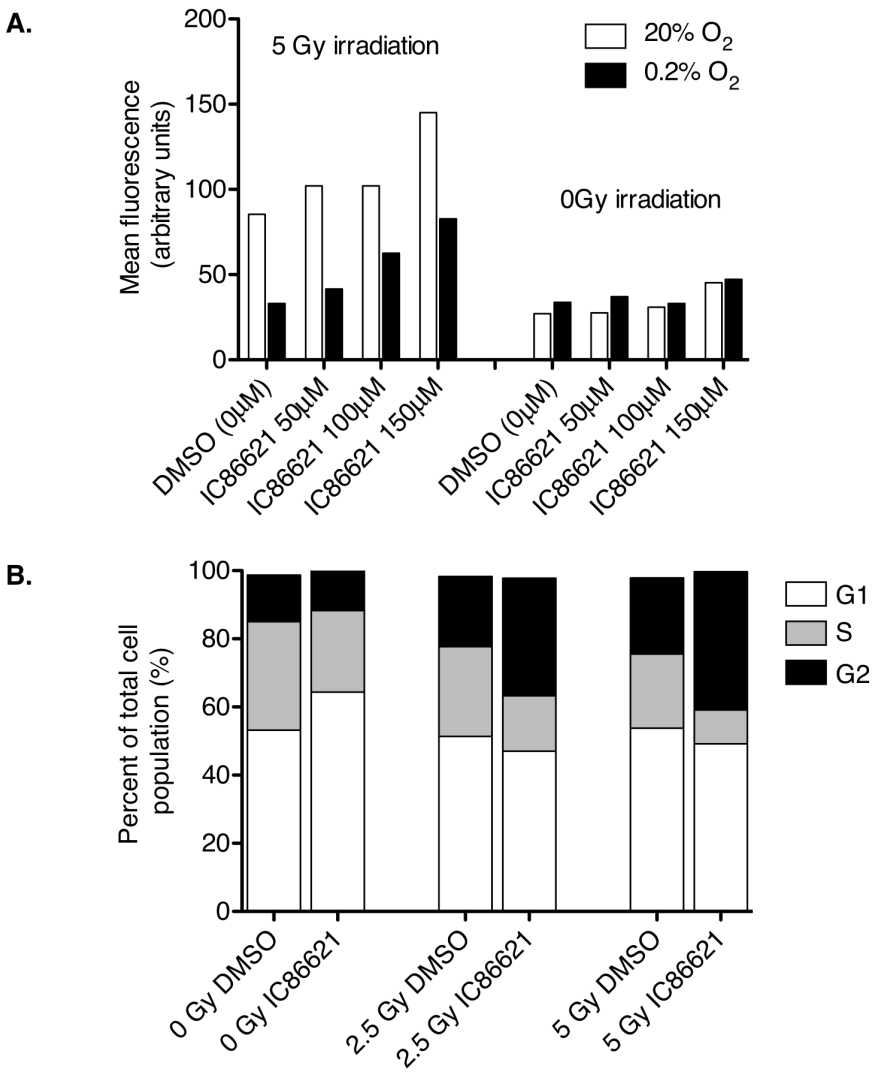


**Figure 4.6 DNA-PK inhibitor IC86621 in combination with ionizing radiation causes an IC86621 dose dependent increase in residual DNA damage and elicits a G2 block.**

A) The mean γH2AX intensity of > 10,000 cells was analyzed by flow cytometry. 24 h following irradiation γH2AX intensity increases along with the concentration of IC86621 in cells treated with 50, 100 or 150 μM IC86621 in combination with 5 Gy IR. This indicates that the DNA-PK inhibitor increases residual DNA damage in cells following IR in an inhibitor dose dependent manner.

B) The proportion of cells in G2 phase of the cell cycle is increased in HeLa cells treated with 100 μM IC86621 in combination with 2.5 or 5 Gy IR versus treatment with IR alone. This result suggests that when DNA-PK is inhibited, a greater proportion of cells have activation of the G2 checkpoint following DNA damaging IR treatment. Shown here is the cell cycle analysis of hypoxic cells from the experiment displayed in figure 4.5A, though similar results were obtained with the oxic cells treated in parallel (data not shown).

## 4.5 IC86621 loses DNA-PK inhibitory activity when modified at the 2-hydroxyl site

### Introduction

The inhibitor IC86621 was chosen as a lead compound for the generation of hypoxia activated DNA-PK inhibitors as it was suspected that the 2'-hydroxyl moiety on IC86621 would provide a suitable site for an ether linkage to the hypoxia activated trigger. This would theoretically allow for reduction of the prodrug as per the proposed scheme in figure 4.7 A.

The binding pocket of DNA-PKcs is predominantly composed of hydrophobic amino acid residues, and correspondingly, many of the more selective inhibitors of DNA-PK contain lipophilic scaffolds. Unfortunately there is no high-resolution structure available for DNA-PKcs, likely due to its very large 470 kDa size, and it is unknown where exactly on the folded protein the ATP binding domain resides. However, DNA-PKcs has a high degree of homology with the ATP binding domain of the structurally well-characterized protein PI-3Kγ. An X-ray diffraction co-crystal structure of PI-3Kγ with the inhibitor LY294002 bound in the ATP binding domain was published by Walker et al. in 2000 (69). Several drug development groups have used LY294002 as a scaffold structure, from which chemical libraries have been designed and screened for DNA-PK inhibitory activity (16, 31).

From the PI-3Kγ -LY294002 co-cystal structure, it has been discerned that a hydrogen bond is formed between the morpholino oxygen of LY294002 and the backbone amide of Val-882(69). As this valine residue is conserved between PI3Kγ and DNA-PKcs, and the morpholino group is a common scaffold between LY294002 and IC86621, it is suspected that the binding of IC86621 to DNA-PKcs is structurally similar to that of PI3Kγ -LY294002, see figure 4.7 B. It was also detected from the Walker at al.

study that there is a putative hydrogen bond between the ketone moiety of LY294002 and the ζN of Lys-833 of PI3Kγ (69). This lysine is also conserved between the ATP binding pockets of PI3Kγ and DNA-PKcs. Interestingly, Walker et al. observed that the space surrounding the ketone moiety of LY294002 is restricted and this ketone moiety is analogous in structure to the 2'-hydroxyl moiety in IC86621, see figure 4.7 B (69). If the binding of IC86621 to DNA-PK is as expected based on structural similarities, this model suggests there to be limited space surrounding the 2'-hydroxyl region on IC86621. This limited space would signify the 2'-hydroxyl site to be ideal for trigger attachment because conjugation of a trigger at this site could provide the steric hindrance necessary to deactivate the effector component of the prodrug, IC86621, until hypoxia mediated fragmentation of the prodrug occurs.

**Approach**

To further investigate whether the 2' hydroxyl site of IC86621 is a good candidate for trigger attachment two analogs of IC86621 were synthesized, each of which is blocked at the 2'hydroxyl site by an O-linkage to a small methyl (HADRI1) and allyl (HADRI2) functional group, see Appendix C. Only HADRI1 was tested for its ability to inhibit DNA-PK by assessing its radiosensitization ability, as HADRI2 had poor aqueous solubility.

HADRI1 was assessed for radiosensitizing ability using the clonogenic survival assay described in section 2.5. As we had previously determined that DNA-PK inhibition sensitizes hypoxic cells and it is expected that the HADRI compound would act similarly under both oxic and hypoxic conditions, for simplicity this assay was performed under normal atmospheric conditions (21% $O_2$). The multi-attenuator insert was used within the aluminium chambers to achieve various does of radiation. However, the cells were not treated with the gas exchange procedure. Triplicate dishes were plated for each

treatment group and the combined results of two experiments are presented with error bars representing the mean ± standard deviation.

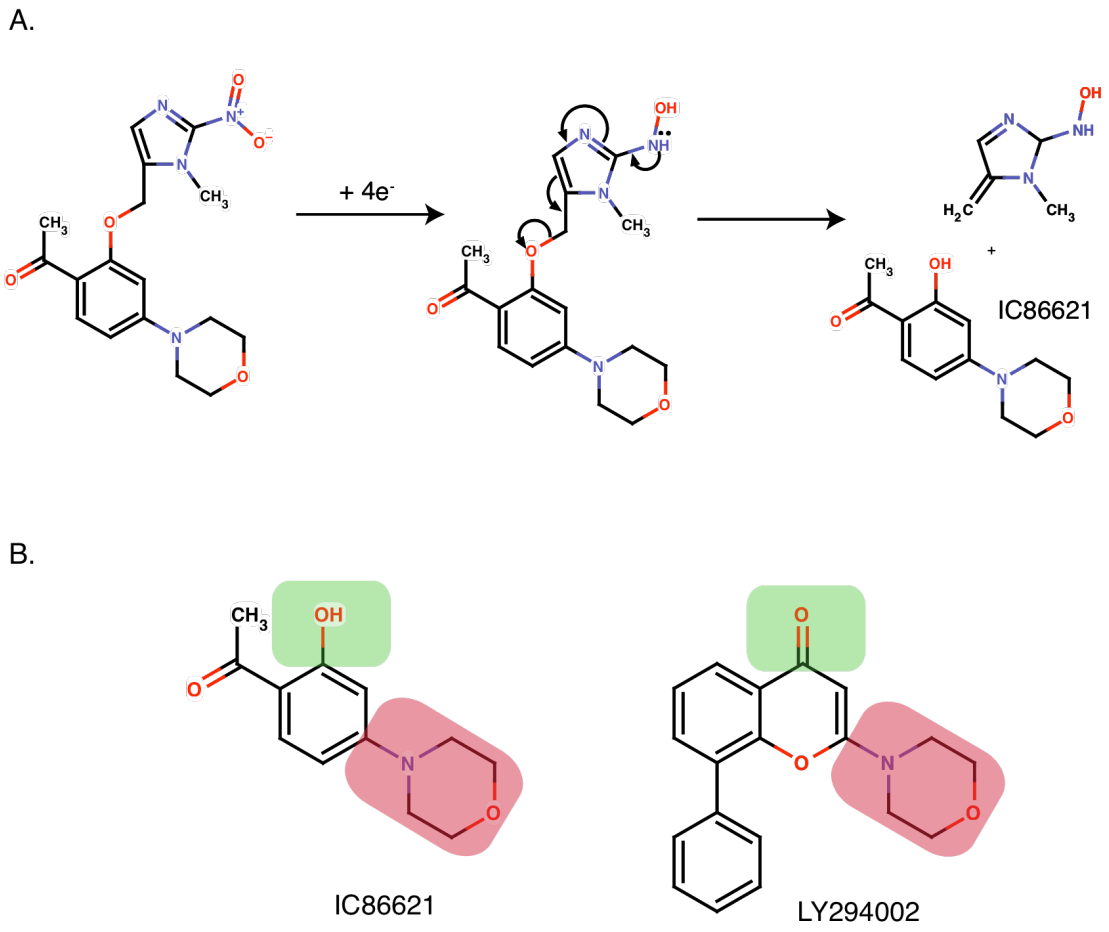


**Figure 4.7 Reduction scheme of HAPI3 in hypoxia and structural comparison of IC86621 to LY294002**

A) A predicted reduction scheme of candidate prodrug HAPI3. Previous studies with nitroimidazole based prodrugs resulting in intramolecular fragmentation have characterized the stepwise bioreduction of a nitroimidazole by a 4 electron reduction into a hydroxylamine. The unstable hydroxylamine prodrug then breaks apart by a through-bond fragmentation of the ether linkage. In the case of HAPI2 and HAPI3, this fragmentation is designed to result in the generation of DNA-PK inhibitor IC86621 in addition to trigger residue by-product.

B) Based upon structural similarity between the inhibitors LY294002 and IC86621 and the PI3Kγ and DNA-PK enzymes, the co-crystal structure of LY294002 bound to PI3Kγ suggests that space surrounding the 2'-hydroxyl moiety of IC86621 in the ATP binding pocket of DNA-PKcs may be limited. If this is the case, then the addition of a bulky hypoxia activated trigger to the 2'-hydroxyl would be likely to sterically hinder access of the prodrug to the ATP binding pocket of DNA-PKcs.

**Results**

The results displayed in figure 4.8 are the average ± standard deviation from two experiments. Treatment with HADRI 1 displayed no radiosensitization over the vehicle control cells treated with 0.14% DMSO, indicating that no inhibition of DNA repair occurs with HADRI1 treatment. Also of note is that no apparent toxicity was observed in treatment with HADRI1 over that of the vehicle control. This result is in accordance with the structural model prediction suggesting the modification at the 2'hydroxyl will impair the DNA-PK inhibitory activity of IC86621. As expected, however, treatment with the unmodified IC86621 in combination with ionizing radiation decreased the surviving fraction of cells at all radiation doses, indicating an inhibition of DNA repair attributable to DNA-PK inhibition.

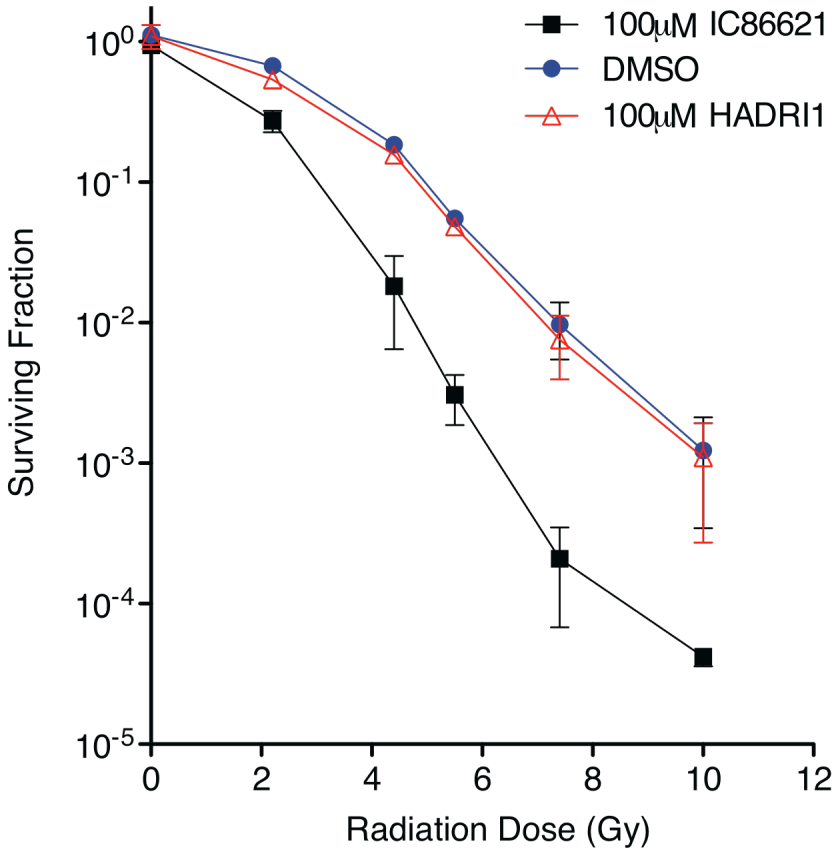


**Figure 4.8 Modification of the 2'- hydroxyl on IC86621 to an O-methyl eliminates radiosensitization activity**

HeLa cells were treated with 100μM IC86621 or 100μM HADRI1 (See Appendix C) in order to determine the relative importance of the 2'hydroxyl group on IC86621 to confer DNA-PK inhibitory activity which results in radiosensitization. A vehicle control treated with 0.14% DMSO was also test. Cells were treated with the drugs hour before irradiation and the drugs remained on for 4h following irradiation.

HADRI1 displays no radiosensitizing ability (△), and has no discernable activity over that of the DMSO control (●). As anticipated however, IC86621 displayed decreased surviving fractions over both HADRI1 and DMSO controls at all radiation doses administered (■). This result points to a critical role for the 2'hydroxyl on IC86621 in DNA-PK inhibition and suggests that the 2'hydroxyl site would be optimal for the addition of a hypoxia activated trigger as it would likely eliminate DNA-PK inhibitory activity in the prodrug form of the compound. Error bars represent the mean ± standard deviation from six interexperiment replicates combined from two experiements each with dishes plated in triplicate.

# Chapter 5: Screening and development

Throughout the development process the cell viability and clonogenic survival screening assays have been refined and have served as useful tools to assess radiation sensitivity under both oxic and hypoxic conditions. We have thereby continued to use these assays for the screening of two of three candidate prodrug compounds.

The first compound synthesized, HAPI1, contained a nitrobenzene trigger moiety, see **Appendix C**. Unfortunately, HAPI1 had poor aqueous solubility and thereby was not thoroughly screened as a part of this work. There is a possibility however that HAPI1 could display promising hypoxia selective radiosensitizing activity and future work could address the opportunity to modify HAPI1 with polar functional groups in order to improve its aqueous solubility.

Results from the preliminary cell-based screening of two other prodrug candidates, HAPI2 and HAPI3, along with *in vitro* screening of HAPI3 with a microsomal stability assay, are presented in this chapter. A majority of this work was done with HAPI3 as the chemical synthesis of HAPI2 was problematic and only a small amount of HAPI2 was available for screening.

## 5.1 Prodrug HAPI2 displays hypoxia selective radiosensitization and dose dependent toxicity under both oxic and hypoxic conditions

### Introduction

Only 3 mg of the 2-nitroimidazole-IC86621 prodrug HAPI2 was synthesised by Dr. Bhaskar Rheddy in Dr. Gregory Dake's laboratory in the UBC Department of

Chemistry. However, results with HAPI2 have been included because this prodrug showed interesting and desirable activity in the resazurin reduction assay, which at a minimum displays further validation of the screening approach and beyond that, the data indicates the potential for candidate prodrug if a higher yielding synthetic route were to be developed in the future.

**Approach**

HAPI2 was screened on CB.17 MEF cells using the resazurin reduction assay as described in section 2.4. It is important to note that this compound was approximately 80% pure by nuclear magnetic resonance analysis and contained unknown impurities that may have affected the experimental results presented below. CB.17 cells were used in this assay because our decision to screen primarily on HeLa cells, which provide a more relevant model of human cancer, had not yet been made. It has been established that human and non-human primate cells have significantly higher expression levels of DNA-PK than mice and other mammals(70). Additionally, as no humans have been known to carry a DNA-PK deficiency, it is suspected that non-functional DNA-PK mutations are embryonic lethal in humans, contrary to other mammals including mice, dogs, and horses(70). Despite these differences, comparable results were obtained between HeLa and CB.17 cells when testing the DNA-PK inhibitors IC86621.

In this experiment HAPI2 was added to the cells at 0, 25, 50, or 100 μM immediately before gassing with 0.2% $O_2$ or 21% $O_2$ gas each containing 5% $CO_2$/ balance $N_2$. The 0 μM treatment contained 0.4% DMSO as a vehicle control such that the volume of DMSO added equalled that of the 100 μM HAPI2 condition. Following gassing, the chambers were incubated for 1 h at 37 °C before irradiation with 5 Gy or mock irradiation. Sealed chambers were then placed in a 37 °C oven for 6 h while cells were allowed to recover from the IR in the presence or absence of HAPI2 and hypoxia.

After 6h the chambers were opened to the air and prodrug-containing media was removed and replaced with fresh media and the 24 well plates were placed under normal incubation conditions. 72 h from the time of IR administration resazurin was added to assess cell viability according to the protocol described in section 2.4.

**Results**

The results of this experiment are presented in figure 5.1. In examining the non-irradiated (0 Gy) treatment groups, the decreasing resorufin signal with increasing doses of HAPI2 clearly displays a dose dependent toxicity for HAPI2 over the concentration range tested in both oxic and hypoxic conditions. However, in cells where DNA damage has been induced by the administration of 5 Gy ionizing radiation, HAPI2 does appear to have hypoxia selective radiosensitizing ability indicated by the dose dependent decrease in resorufin fluorescence only under hypoxic conditions. We were surprised to find slightly lower viability in the hypoxic cells compared to oxic cells in both the non-irradiated and irradiated cells. However, upon investigation of the experimental protocol it became clear that during incubation the hypoxic chambers were heated up to a temperature above 37 °C, which likely accounts for the overall decreased viability of the hypoxic cells and cannot be ruled out as a confounding factor. The results presented with HAPI2 are representative of three independent experiments. Unfortunately, due to the small amount of HAPI2 available we have been unable to repeat this experiment with appropriate incubation conditions.

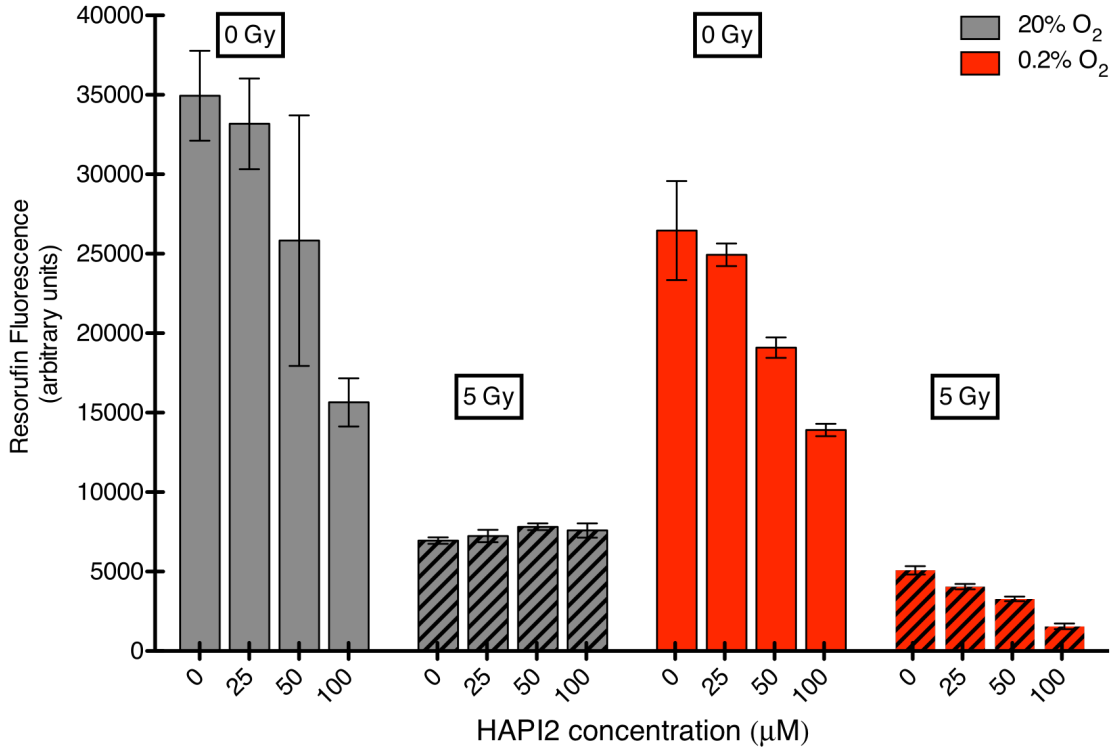


**Figure 5.1 HAPI2 displays dose dependent hypoxia selective radiosensitizing ability**

CB.17 cells were pre-treated for 1h with 25-100 μM of the candidate prodrug HAPI2 in combination with either 20% $O_2$ (oxic conditions) or 0.2% $O_2$ (hypoxic conditions). After 1 h the cells were irradiated with 5 Gy or mock irradiated for the 0Gy condition. Following irradiation cells remained within the hypoxia chambers and were allowed to recover for 6 h in the presence of the prodrug. After 6 h cells were removed, the prodrug was removed and cells were allowed to recover for a further 72h in the normal incubation conditions before cell viability was assessed with the resazurin reduction assay.

HAPI2 causes a dose dependent toxicity under both oxic and hypoxic conditions in the absence of radiation (grey and red solid bars). When DNA damage is induced with 5 Gy ionizing radiation, HAPI2 caused a similar dose dependent toxicity selectively under hypoxic conditions (red striped versus grey striped bars). This result suggests reduction of the prodrug HAPI2 into the DNA-PK inhibitor IC86621 occurred selectively under hypoxic conditions.

No oxygen enhancement ratio was observed in this experiement. During the 6h drug exposure following radaition or mock radiation administration the hypoxic aluminium chambers, were accidently over heated. Cell death due to the excess heat likely explains the overall decreased viability of the hypoxic cells in this experiement, but probably does not account for the effect of the HAPI2 prodrug.

## 5.2 Prodrug HAPI3 decreases cell viability selectively in hypoxic cells treated with ionizing radiation

### Introduction

The third candidate prodrug to be synthesized, HAPI3, is structurally very similar to HAPI2, with the exception of an additional methyl group attached at the 1-position on the imidazole ring. A synthetic route for this compound was developed by members of Dr. Gregory Dake's laboratory at the UBC Department of Chemistry and was further optimized by Geoff Winters at the Centre for Drug Research and Development (Vancouver, Canada).

### Approach

In this experiment HAPI3 was added to HeLa cells at 0, 25, 50, 100 or 150 μM immediately before gassing with 0% $O_2$, hypoxic conditions, or 21% $O_2$, oxic conditions, with each gas containing 5% $CO_2$/ balance $N_2$. The 0 μM treatment group contained 1% DMSO as a vehicle control such that the volume of DMSO equalled that of the 150 μM HAPI3 treatment. Additionally included are cells treated with 100 μM IC86621 for comparison as a positive control of radiosensitization. Following gassing, the chambers were incubated for 1 h at 37 °C before the chambers receiving radiation were treated with either 5 Gy (oxic cells) or 12.5 Gy (hypoxic cells). In this experiment the hypoxic cells were treated with a dose of radiation 2.5x higher than that of the oxic cells in order to achieve approximately equal cell kill between the two conditions. Chambers were then returned to the 37 °C oven for 4 h while cells were allowed to recover in the presence or absence of HAPI2 and hypoxia. After 4 h the chambers were opened to the air and the prodrug containing media was removed and replaced with 500 μL fresh media. The cells

were then allowed to recover for a further 72 h under normal incubation conditions before resazurin was added to assess cell viability as per section 2.4.

**Results**

Figure 5.2 displays the results of both the irradiated and non-irradiated cells in the screen. As expected, IC86621 displays no obvious toxicity in the absence of DNA damage. However both oxic and hypoxic cells are sensitized to ionizing radiation by the DNA-PK inhibitor. As per the experimental design, hypoxic DMSO control cells irradiated at 12.5 Gy were found to have similar, albeit slightly increased viability 72 h following irradiation compared to oxic DMSO control cells irradiated with 5 Gy. Equalizing the cell viability between the oxic and hypoxic cells eases comparison between these treatment groups, while also showing that the hypoxic cells are resistant to the effects of radiation. In contrast to HAPI2, no obvious off target toxicity was observed in the non-irradiated cells treated with 25-100 μM HAPI3. However, with 150 μM HAPI3 treatment cell viability did decrease somewhat in both oxic and hypoxic cells. As displayed in figure 5.3, increasing concentrations of HAPI3 beyond 25 μM were found to cause dose dependent radiosensitization *selectively in hypoxic cells*. Figure 5.3 displays results from the same screening assay, however in this figure only the irradiated treatment groups are displayed and individual replicates are plotted. As these preliminary screening results display the desired hypoxia selective radiosensitizing activity, and because sufficiently more of the HAPI3 compound has been made available for screening, future work with HAPI3 will include clonogenic survival assays and potentially anti-cancer activity and pharmacological evaluation in mice.

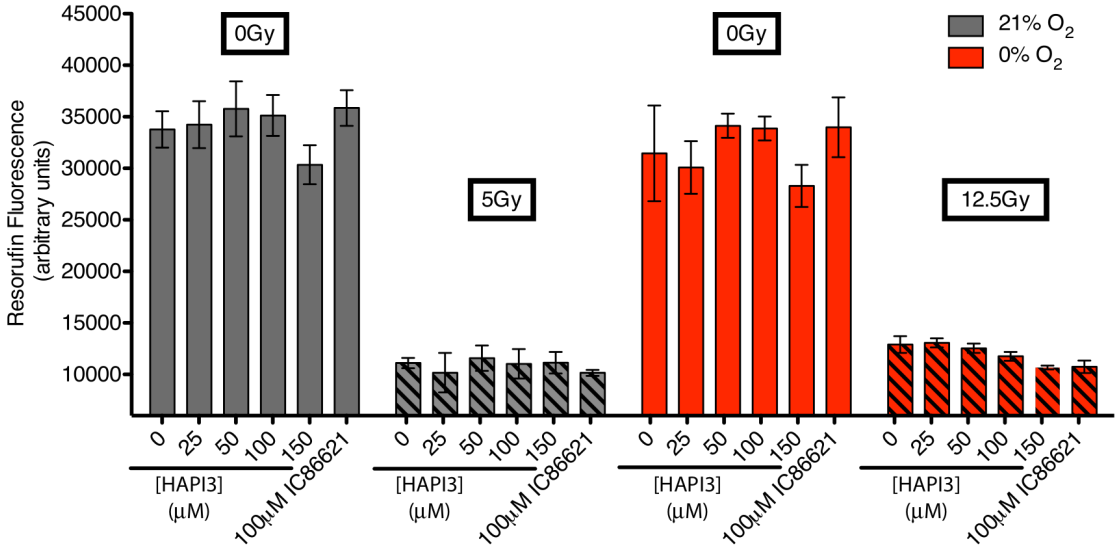


**Figure 5.2 HAPI3 displays no off-target toxicity in the 25-100μM range**

Oxic (21% $O_2$) and hypoxic (0% $O_2$) HeLa cells were pre-treated for 1h with 0-150 μM HAPI3 or 100 μM IC86621. The 0 μM HAPI3 treatment contained 1% DMSO as a vehicle control. After 1 h cells were administered 5 Gy (oxic cells), 12.5 Gy (hypoxic cells) or non-irradiated cells were left for continued incubation (0 Gy). Drug treatments remained on the cells for 4 h following irradiation. Cells were allowed to recover under normal incubation conditions for 72 h before cell viability was assessed with the resazurin reduction assay.

In the absence of radiation HAPI3 causes no obvious toxicity in the 25-100 μM range in either oxic or hypoxic cells, however at 150 μM a slight decrease in cell viability is observed in both the hypoxic and oxic non-irradiated cells. Irradiated cells within the oxic vehicle control treatment group (first grey striped bar) have slightly lower viability than the irradiated vehicle control hypoxic cells (red striped bars), indicating an OER >2.5 has been reached (OER >12.5 Gy/5 Gy).

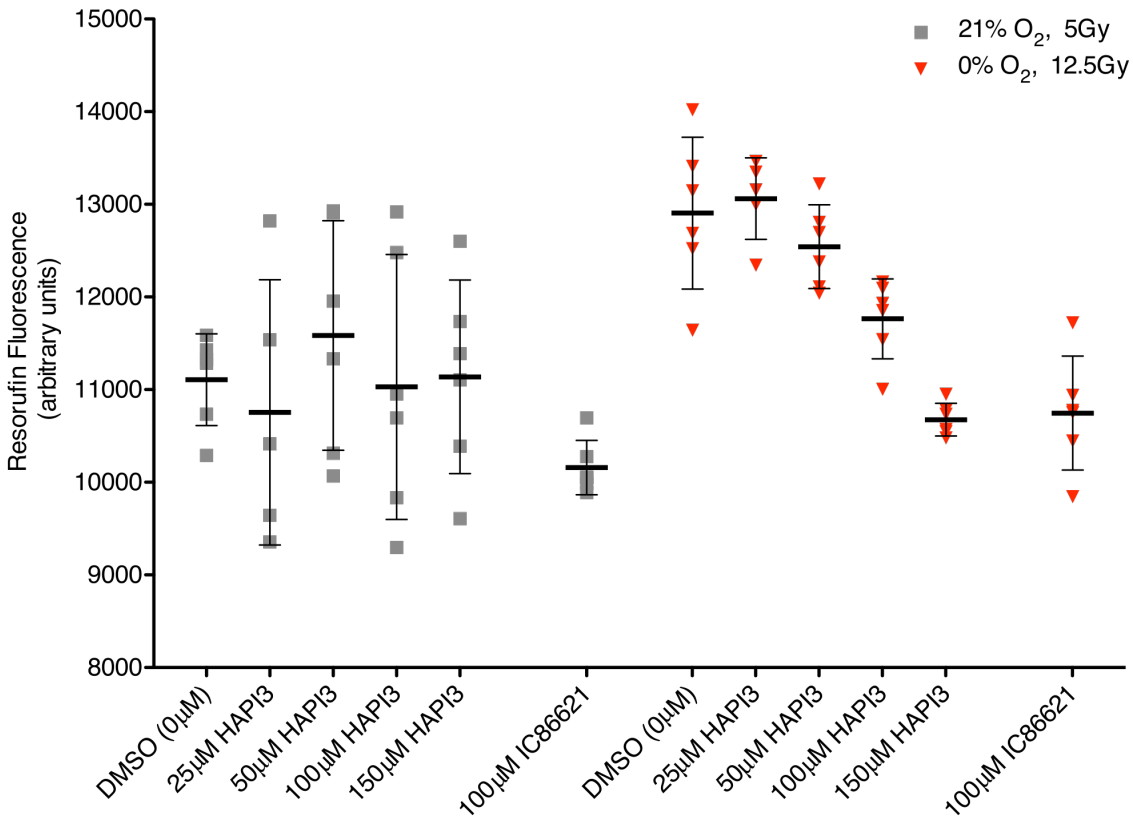


**Figure 5.3 HAPI3 has activity as a hypoxia selective radiosensitizer**

Data displayed is the same as that in Figure 5.2, except that the non-irradiated cells have been omitted and the scale is fitted to gain a closer look at the irradiated cells. Here each symbol represents an individual well from a 24-well plate and the mean ± standard deviation from 6 replicate wells is displayed. Following 5Gy irradiation in oxic cells HAPI3 causes no net effect at any of concentrations tested, however a larger inter replicate viability is noted. In contrast, 100μM IC86621 causes decreased cell viability in concordance with its DNA-PK inhibitory activity. In hypoxic cells IC86621 also causes decreased cell viability, however in hypoxic cells HAPI3 displays radiosensitizing activity in a dose dependent manner, and less inter replicate variability is apparent.

## 5.3 Prodrug HAPI3 is reduced by an NADPH dependent enzyme to the DNA-PK inhibitor IC86621 selectively under hypoxic conditions

### Introduction

To assess activity of candidate prodrugs more mechanistically we have employed a cell-free microsomal stability assay. Microsomes are vesicular artifacts from the endoplasmic reticulum of lysed eukaryotic cells that are rich in metabolic enzymes (42). Liver microsomal stability is often used under normoxic conditions in drug development efforts to estimate the extent of hepatic metabolism a compound will undergo *in vivo* (42). However, for our purposes microsomal stability is assessed under both oxic and hypoxic circumstances to measure differences in the bioreduction products formed from hypoxia activated prodrug candidates.

### Approach

Details of mouse liver microsome preparations and prodrug incubations are described in section 2.7. High pressure liquid chromatography was used to separate the parent prodrug HAPI3 from the reduction product IC86621 (see section 2.8 for details). Incubations were performed in triplicate and error bars displayed represent the mean ± standard deviation.

### Results

The concentration of prodrug HAPI3 and the DNA-PK inhibitor IC86621 are plotted against microsomal incubation time in figure 5.4 A, B. During incubation in the presence of NADPH, seen in figure 5.4A, under atmospheric oxygen the concentration of HAPI3 decreases from 34 to 16 μM over 2 h, indicating microsomal enzyme mediated metabolism of the prodrug. However, only a small amount of this metabolism resulted in

the production of IC86621, the concentration of which increased only slightly from 0 to 1 μM over the same 2 h time period. This result is in contrast to that obtained from performing the same assay under hypoxic conditions. In hypoxia, HAPI3 was more rapidly metabolized, falling from 30 to 1.5 μM over 2 h. Also, in hypoxia the reduction product IC86621 was favoured, with up to 18 μM IC86621 being formed over 2 h. This result suggests that the reduction scheme proposed in figure 4.7A is likely to be occurring. However, because an incomplete yield of HAPI3 to IC86621 resulted, additional metabolic processes which do not result in IC86621 are also apparent. Although a number of different enzymes have been found to be involved with the reduction of hypoxia activated prodrugs, the primary enzyme for 2-nitroimidazole bioreduction has been shown to be NADPH-dependent cytochrome P450 reductase (71, 72). Our results are consistent with NADPH-dependent P450 reductase metabolism in that little to no reduction of the prodrug or generation of IC86621 was observed in the absence of NADPH (see figure 5.4 B).

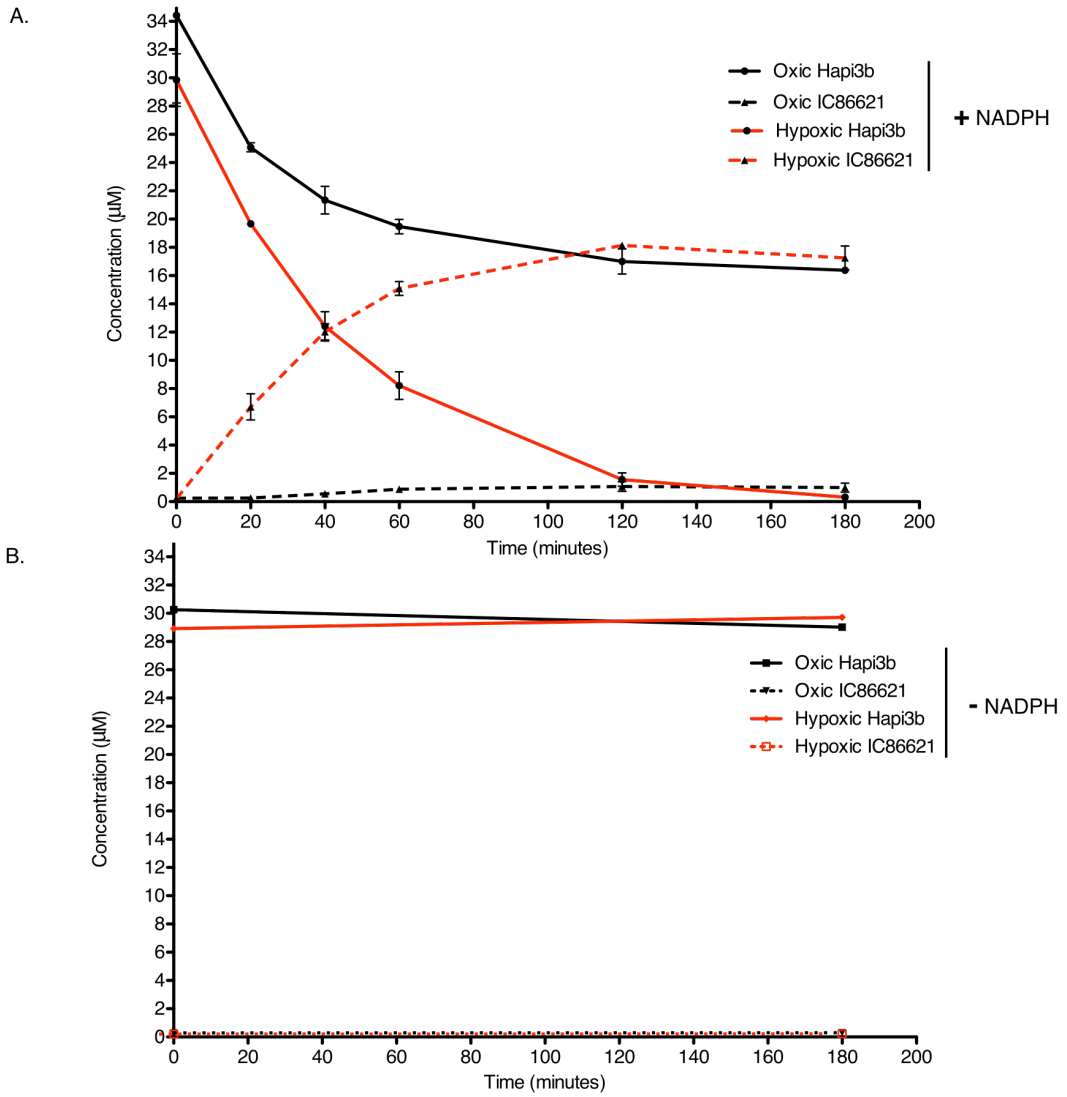


Figure 5.4 Bioreduction of HAPI3 by liver microsomes require NADPH and selectively produces IC86621 under hypoxic conditions

A) The concentration of HAPI3 (solid lines) and IC86621 (dashed lines) was followed over time throughout incubation with mouse liver microsomes in oxic and hypoxic conditions. In the presence of NADPH and 21%$O_2$, the concentration of prodrug HAPI3 decreases over time as it metabolized by the microsomal enzymes. However, very little IC86621 results from the metabolism of HAPI3 under oxic conditions, with less than 1µM IC86621 produced after 2h. In 0.2% $O_2$ conditions, HAPI3 is more rapidly metabolized, with less than 1µM present after 2h and in contrast to the oxic conditions, IC86621 is selectively produced from this metabolism, with 18µM IC86621 present after 2h. These results suggest that the proposed intramolecular fragmentation of HAPI3 in to IC86621 is occurring selectively under hypoxic conditions and that the enzyme(s) responsible for reduction of the prodrug are NADPH dependent.

B) In the absence of the NADPH enzyme cofactor HAPI3 is not converted into IC86621 and no apparent degradation of the prodrug occurs over the 180min microsome incubation in either oxic or hypoxic conditions (solid lines). The concentration of IC86621 remains stable at <0.25µM. This small amount of IC86621 represents the fraction present in the stock solution of HAPI3.

# References


1. Helleday T, Petermann E, Lundin C, Hodgson B, Sharma R. DNA repair pathways as targets for cancer therapy. Nat Rev Cancer 2008.

2. Chadwick KH, Leenhouts HP. A molecular theory of cell survival. Physics in medicine and biology; 1973. p. 78-87.

3. Dugle DL, Gillespie CJ, Chapman JD. DNA strand breaks, repair, and survival in x-irradiated mammalian cells. Proc Natl Acad Sci USA; 1976. p. 809-12.

4. Thacker J, Zdzienicka MZ. The XRCC genes: expanding roles in DNA double-strand break repair. DNA Repair (Amst) 2004; 3: 1081-90.

5. Alexander P. On the mode of action of some treatments that influence the radiation sensitivity of cells. Transactions of the New York Academy of Sciences 1962; 4: 966-78.

6. Murray D, Mirzayans R, Scott AL, Allalunis-Turner MJ. Influence of oxygen on the radiosensitivity of human glioma cell lines. Am J Clin Oncol 2003; 26: e169-77.

7. Helleday T, Lo J, van Gent DC, Engelward BP. DNA double-strand break repair: from mechanistic understanding to cancer treatment. DNA Repair (Amst) 2007; 6: 923-35.

8. Huertas P, Cortés-Ledesma F, Sartori AA, Aguilera A, Jackson SP. CDK targets Sae2 to control DNA-end resection and homologous recombination. Nature; 2008. p. 689-92.

9. Chan N, Koritzinsky M, Zhao H, et al. Chronic hypoxia decreases synthesis of homologous recombination proteins to offset chemoresistance and radioresistance. Cancer Res 2008; 68: 605-14.

10. Bindra RS, Schaffer PJ, Meng AX, et al. Alterations in DNA Repair Gene Expression under Hypoxia: Elucidating the Mechanisms of Hypoxia-Induced Genetic Instability. Ann NY Acad Sci; 2005. p. 184-95

11. Bristow RG, Hill RP. Hypoxia and metabolism: Hypoxia, DNA repair and genetic instability. Nat Rev Cancer; 2008.

12. Mahaney BL, Meek K, Lees-Miller SP. Repair of ionizing radiation-induced DNA double-strand breaks by non-homologous end-joining. Biochem J 2009; 417: 639-50.

13. Walker JR, Corpina RA, Goldberg J. Structure of the Ku heterodimer bound to DNA and its implications for double-strand break repair. Nature 2001; 412: 607-14.

14. Meek K, Douglas P, Cui X, Ding Q, Lees-Miller SP. trans Autophosphorylation at DNA-dependent protein kinase's two major autophosphorylation site clusters facilitates end processing but not end joining. Mol Cell Biol 2007; 27: 3881-90.

15. Lovejoy CA, Cortez D. Common mechanisms of PIKK regulation. DNA Repair 2009; 8: 1004-8.

16. Hollick JJ, Rigoreau LJM, Cano-Soumillac C, et al. Pyranone, Thiopyranone, and Pyridone Inhibitors of Phosphatidylinositol 3-Kinase Related Kinases. Structure-Activity Relationships for DNA-Dependent Protein Kinase Inhibition, and Identification of the First Potent and Selective Inhibitor of the Ataxia Telangiectasia Mutated Kinase. J Med Chem 2007; 50: 1958-72.

17. Williams DR, Lee KJ, Shi J, Chen DJ, Stewart PL. Cryo-EM structure of the DNA-dependent protein kinase catalytic subunit at subnanometer resolution reveals alpha helices and insight into DNA binding. Structure 2008; 16: 468-77.

18. Moeller BJ, Richardson RA, Dewhirst MW. Hypoxia and radiotherapy: opportunities for improved outcomes in cancer treatment. Cancer Metastasis Rev 2007; 26: 241-8.

19. Overgaard J. Hypoxic radiosensitization: adored and ignored. J Clin Oncol 2007; 25: 4066-74.

20. Overgaard J. Clinical evaluation of nitroimidazoles as modifiers of hypoxia in solid tumors. Oncol Res 1994; 6: 509-18.

21. Overgaard J, Horsman MR. Modification of hypoxia-induced radioresistance in tumors by the use of oxygen and sensitizers. Semin Radiat Oncol 1996; 6: 10-21.

22. Bennett M, Feldmeier J, Smee R, Milross C. Hyperbaric oxygenation for tumour sensitisation to radiotherapy: a systematic review of randomised controlled trials. Cancer Treat Rev 2008; 34: 577-91.

23. Wardman P. Chemical radiosensitizers for use in radiotherapy. Clin Oncol (R Coll Radiol) 2007; 19: 397-417.

24. Varghese AJ, Whitmore GF. Detection of a reactive metabolite of misonidazole in human urine. Int J Radiat Oncol Biol Phys 1984; 10: 1361-3.

25. Varghese AJ, Whitmore GF. Binding to cellular macromolecules as a possible mechanism for the cytotoxicity of misonidazole. Cancer Res 1980; 40: 2165-9.

26. Rich TA, Dische S, Saunders MI, Stratford MR, Minchinton A. A serial study of the concentration of misonidazole in human tumors correlated with histologic structure. Int J Radiat Oncol Biol Phys 1981; 7: 197-203.

27. Skarsgard LD. Radiosensitizing and Toxic Effects of the 2-Nitroimidazole Ro-07-0582 in Hypoxic Mammalian Cells. Radiat Res 1976; 67: 459-73.

28. Denny WA, Wilson WR, Hay MP. Recent developments in the design of bioreductive drugs. Br J Cancer Suppl 1996; 27: S32-8.

29. Everett SA, Naylor MA, Patel KB, Stratford MR, Wardman P. Bioreductively-activated prodrugs for targeting hypoxic tissues: elimination of aspirin from 2-nitroimidazole derivatives. Bioorg Med Chem Lett 1999; 9: 1267-72.

30. Fong PC, Boss DS, Yap TA, et al. Inhibition of poly(ADP-ribose) polymerase in tumors from BRCA mutation carriers. N Engl J Med 2009; 361: 123-34.

31. Kashishian A, Douangpanya H, Clark D, et al. DNA-dependent protein kinase inhibitors as drug candidates for the treatment of cancer. Mol Cancer Ther 2003; 2: 1257-64.

32. Shinohara ET, Geng L, Tan J, et al. DNA-dependent protein kinase is a molecular target for the development of noncytotoxic radiation-sensitizing drugs. Cancer Res 2005; 65: 4987-92.

33. Leahy JJ, Golding BT, Griffin RJ, et al. Identification of a highly potent and selective DNA-dependent protein kinase (DNA-PK) inhibitor (NU7441) by screening of chromenone libraries. Bioorg Med Chem Lett 2004; 14: 6083-7.

34. Ismail IH, Susanne M, Moshinsky D, Rice A, Tang C. SU11752 inhibits the DNA-dependent protein kinase and DNA double-strand break repair resulting in …. Oncogene 2004.

35. O'Connor MJ, Martin NM, Smith GCM. Targeted cancer therapies based on the inhibition of DNA strand break repair. Oncogene 2007; 26: 7816-24.

36. Durant S, Karran P. Vanillins--a novel family of DNA-PK inhibitors. Nucleic Acids Res 2003; 31: 5501-12.

37. Allen C, Halbrook J, Nickoloff JA. Interactive competition between homologous recombination and non-homologous end joining. Mol Cancer Res 2003; 1: 913-20.

38. Convery E, Shin EK, Ding Q, et al. Inhibition of homologous recombination by variants of the catalytic subunit of the DNA-dependent protein kinase (DNA-PKcs). Proc Natl Acad Sci USA 2005; 102: 1345-50.

39. Koch CJ. A thin-film culturing technique allowing rapid gas-liquid equilibration (6 sec) with no toxicity to mammalian cells. Radiat Res; 1984. p. 434-42.

40. Halbrook J, Kesicki EA, Burgess LE, et al., inventors; Luitpold Pharmaceuticals Inc., assignee. Materials and Methods to Potentiate Cancer Treatment. United States patent US 2008/0090782 A1. 2008 Apr. 17, 2008.

41. Anoopkumar-Dukie S. Resazurin assay of radiation response in cultured cells. British Journal of Radiology 2005; 78: 945-7.

42. Wu W, McKown L. In Vitro Drug Metabolite Profiling Using Hepatic S9 and Human Liver Microsomes. … Drug Discovery: In Vitro Methods 2004.

43. Kaizerman J, Stanton T, Evans J, Lan L. … highly selective hypoxia-activated achiral phosphoramidate mustards as anticancer drugs. J Med Chem 2008.

44. Cameron JK, Painter RB. The Effect of Extreme Hypoxia on the Repair of DNA Single-Strand Breaks in Mammalian Cells. Radiation Research 1975; 64: 256-69.

45. Popovici RM, Lu M, Bhatia S, Faessen GH, Giaccia AJ, Giudice LC. Hypoxia regulates insulin-like growth factor-binding protein 1 in human fetal hepatocytes in primary culture: suggestive molecular mechanisms for in utero fetal growth restriction caused by uteroplacental insufficiency. J Clin Endocrinol Metab 2001; 86: 2653-9.

46. Ng CE, Koch CJ, Inch WR. Buoyant density of EMT6 fibrosarcoma cells: time course of the density changes after growth in hypoxia. Cell Biophys 1980; 2: 153-63.

47. Papandreou I, Krishna C, Kaper F, Cai D, Giaccia AJ, Denko NC. Anoxia is necessary for tumor cell toxicity caused by a low-oxygen environment. Cancer Res 2005; 65: 3171-8.

48. Weidemann A, Johnson RS. Biology of HIF-1alpha. Cell Death Differ 2008; 15: 621-7.

49. Meng AX, Jalali F, Cuddihy A, et al. Hypoxia down-regulates DNA double strand break repair gene expression in prostate cancer cells. Radiotherapy and oncology : journal of the European Society for Therapeutic Radiology and Oncology 2005; 76: 168-76.

50. Um JH, Kang CD, Bae JH, et al. Association of DNA-dependent protein kinase with hypoxia inducible factor-1 and its implication in resistance to anticancer drugs in hypoxic tumor cells. Exp Mol Med 2004; 36: 233-42.

51. Ginouvès A, Ilc K, Macías N, Pouysségur J, Berra E. PHDs overactivation during chronic hypoxia "desensitizes" HIFalpha and protects cells from necrosis. Proc Natl Acad Sci USA 2008; 105: 4745-50.

52. Zhao Y, Thomas HD, Batey MA, et al. Preclinical evaluation of a potent novel DNA-dependent protein kinase inhibitor NU7441. Cancer Res 2006; 66: 5354-62.

53. Nutley BP, Smith NF, Hayes A, et al. Preclinical pharmacokinetics and metabolism of a novel prototype DNA-PK inhibitor NU7026. Br J Cancer 2005; 93: 1011-8.

54. Cowell IG, Durkacz BW, Tilby MJ. Sensitization of breast carcinoma cells to ionizing radiation by small molecule inhibitors of DNA-dependent protein kinase and ataxia telangiectsia mutated. Biochem Pharmacol 2005; 71: 13-20.

55. He F, Li L, Kim D, et al. Adenovirus-mediated expression of a dominant negative Ku70 fragment radiosensitizes human tumor cells under aerobic and hypoxic conditions. Cancer Res 2007; 67: 634-42.

56. Kirchgessner CU, Patil CK, Evans JW, et al. DNA-dependent kinase (p350) as a candidate gene for the murine SCID defect. Science 1995; 267: 1178-83.

57. Blunt T, Gell D, Fox M, et al. Identification of a nonsense mutation in the carboxyl-terminal region of DNA-dependent protein kinase catalytic subunit in the scid mouse. Proc Natl Acad Sci USA 1996; 93: 10285-90.

58. Nutley BP, Smith NF, Hayes A, et al. Preclinical pharmacokinetics and metabolism of a novel prototype DNA-PK inhibitor NU7026. Br J Cancer 2005; 93: 1011-8.

59. Stewart R. Two-Lesion Kinetic Model of Double-Strand Break Rejoining and Cell Killing. Radiation Research 2001; 156: 365-78.

60. Botchway S, Stevens D, Hill M, Jenner T, O'Neill P. Induction and Rejoining of DNA Double-Strand Breaks in Chinese Hamster V79-4 Cells Irradiated with Characteristic Aluminum K and Copper L Ultrasoft X Rays. Radiation Research 1997; 148: 317-24.

61. Gauter B, Zlobinskaya O, Weber K-J. Rejoining of Radiation-Induced DNA Double-Strand Breaks: Pulsed-Field Electrophoresis Analysis of Fragment Size Distributions after Incubation for Repair. Radiation Research 2002; 157: 721-33.

62. Bonner WM, Redon CE, Dickey JS, et al. GammaH2AX and cancer. Nat Rev Cancer 2008; 8: 957-67.

63. MacPhail SH, Banáth JP, Yu TY, Chu EH, Lambur H, Olive PL. Expression of phosphorylated histone H2AX in cultured cell lines following exposure to X-rays. International Journal of Radiation Biology 2003; 79: 351-8.

64. Liu SK, Olive PL, Bristow RG. Biomarkers for DNA DSB inhibitors and radiotherapy clinical trials. Cancer Metastasis Rev; 2008.

65. Stiff T, O'Driscoll M, Rief N, Iwabuchi K, Löbrich M, Jeggo PA. ATM and DNA-PK function redundantly to phosphorylate H2AX after exposure to ionizing radiation. Cancer Res 2004; 64: 2390-6.

66. Burma S, Chen BP, Murphy M, Kurimasa A, Chen DJ. ATM phosphorylates histone H2AX in response to DNA double-strand breaks. J Biol Chem 2001; 276: 42462-7.

67. Bucher N, Britten CD. G2 checkpoint abrogation and checkpoint kinase-1 targeting in the treatment of cancer. Br J Cancer 2008; 98: 523-8.

68. Cantley L. The phosphoinositide 3-kinase pathway. Science 2002; 296: 1655.

69. Walker EH, Pacold ME, Perisic O, et al. Structural determinants of phosphoinositide 3-kinase inhibition by wortmannin, LY294002, quercetin, myricetin, and staurosporine. Mol Cell 2000; 6: 909-19.

70. Meek K, Jutkowitz A, Allen L, et al. SCID dogs: similar transplant potential but distinct intra-uterine growth defects and premature replicative senescence compared with SCID mice. J Immunol 2009; 183: 2529-36.

71. Joseph P, JaiswalL A, Stobbe C, Chapman J. The role of specific reductases in the intracellular activation and binding of 2-nitroimidazoles. Int J Radiat Oncol 1994; 29: 351-5.

72. Adams G. Redox, Radiation, and Reductive Bioactivation. Radiation Research 1992; 132: 129-39.

# Appendices

## Appendix A: Chemical structures of various DNA-PK inhibitors

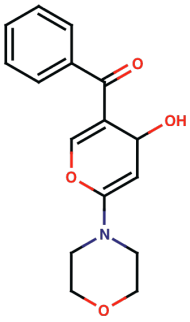


AMA-37

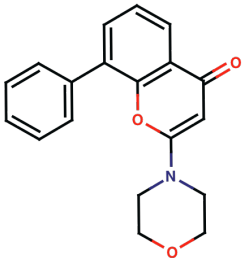


LY294002

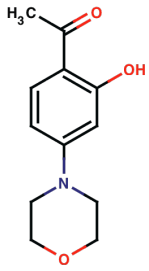


IC86621

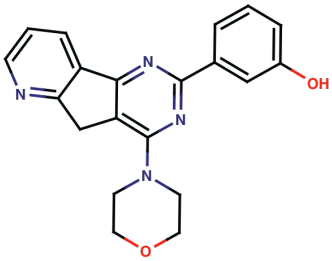


PI-103

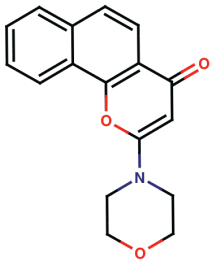


NU7026

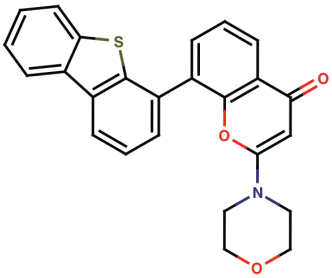


NU7441

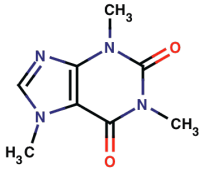


Caffeine

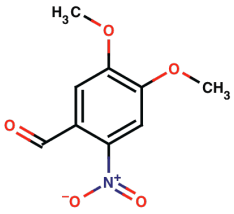


DMNB

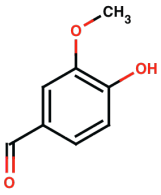


Vanillin

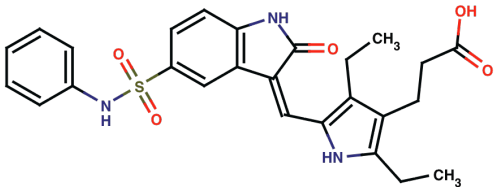


SU11752

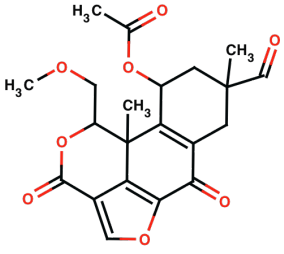


Wortmannin

**Appendix B: Published IC50 values of various DNA-PK inhibitors against PIKK and PI3K family members**

| Inhibitor common name | $IC_{50}$ (μM) | | | | | | | |
|---|---|---|---|---|---|---|---|---|
| | DNA-PKcs | ATM | ATR | mTOR | P110a | P110b | P110d | P110g |
| **PI-103**[1] | 0.002 | 0.92 | 0.85 | ND | 8 | 88 | 48 | 150 |
| **NU7441**[2] | 0.014 | >100 | >100 | 1.7 | 5 | ND | ND | ND |
| **SU11752**[3] | 0.13 | ND | ND | ND | ND | ND | ND | 1.1 |
| **IC86621**[4] | 0.17 | >100 | ND | >100 | 16 | 0.99 | 3.8 | 10 |
| **NU7026**[2] | 0.23 | >100 | >100 | 6.4 | 13 | ND | ND | ND |
| **AMA37**[4] | 0.27 | >100 | >100 | >100 | 32 | 3.7 | 22 | ~100 |
| **Caffeine**[5,6] | ~0.4 | 0.2 | 1.1 | ND | 400 | 400 | 75 | 1000 |
| **LY294002**[4] | 0.66 | >100 | >100 | 8.9 | 9.3 | 2.9 | 6 | 38 |
| **DMNB**[7] | 15 | ND | ND | ND | ND | ND | ND | ND |
| **Vanillin**[6] | ~1500 | ND | ND | ND | ND | ND | ND | ND |
| **Wortmannin**[8,9] | 0.016/ 0.25* | 0.15 | 1.8 | ND | 0.003 | 0.003 | 0.003 | 0.003 |

***** Published values for DNA-PKcs inhibition by wortmannin are variable.

[1] Knight et al. Cell (2006) vol. 125 (4) pp. 733-47
[2] Leahy et al. Bioorg. Med. Chem. Lett. (2004) vol. 14 pp. 6083–6087
[3] Ismail et al. Oncogene (2004) vol. 23 pp. 873–882
[4] Knight et al. Bioorg. Med. Chem (2004) vol. 12 pp. 4749–4759
[5] Block et al. Nucleic Acids Res (2004) vol. 32 (6) pp. 1967-72
[6] Foukas et al. J Biol Chem (2002) vol. 277 (40) pp. 37124-30
[7] Durant et al. Nucleic Acids Res (2003) vol. 31 (19) pp. 5501-12
[8] Sarkaria et al. Cancer Res (1998) vol. 58 (19) pp. 4375-82
[9] Izzard et al. Cancer Res (1999) vol. 59 (11) pp. 2581-6

**Appendix C: Chemical structures and table of common and International Union of Pure and Applied Chemistry names for compounds synthesised as part of the HADRI project**

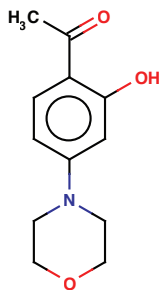


IC86621

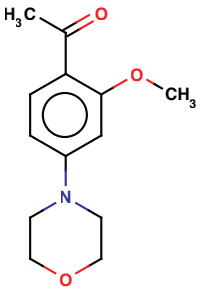


HADRI1

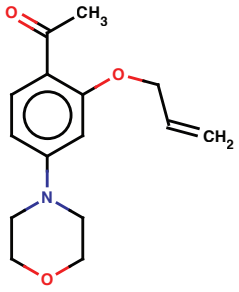


HADRI2

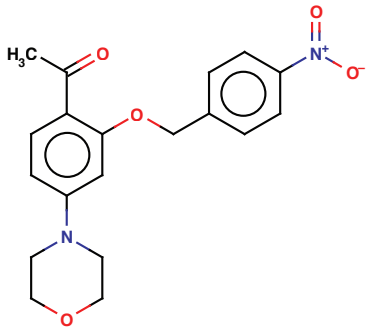


HAPI1

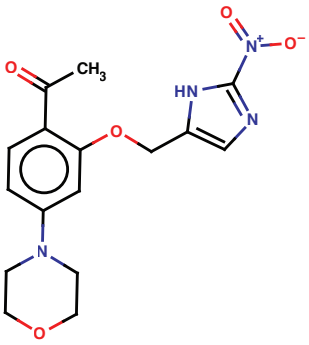


HAPI2

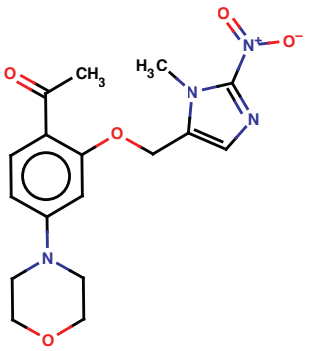


HAPI3

| Common name | International union of pure and applied chemistry (IUPAC) name |
|---|---|
| **IC86621** | 1-(2-Hydroxy-4-morpholin-4-yl-phenyl)ethanone |
| **HADRI 1** | 1-[2-methoxy-4-(morpholin-4-yl)phenyl)ethan-1-one |
| **HADRI 2** | 1-[4-(morpholin-4-yl)-2-(prop-2-en-1-yloxy)phenyl]ethan-1-one |
| **HAPI 1** | 1-[4-(morpholin-4-yl)-2-[(4-nitrophenyl)methoxy]phenyl)ethan-1-one |
| **HAPI 2** | 1-[4-(morpholin-4-yl)-2-[(2-nitro-1H-imidazol-5-yl)methoxy]phenyl]ethan-1-one |
| **HAPI 3** | 1-{2-[(1-methyl-2-nitro-1H-imidazole-5-yl)methoxy]-4-(morpholin-4-yl)phenyl}ethan-1-one |